Nucleated polymerization with secondary pathways. II. Determination of self-consistent solutions to growth processes described by non-linear master equations

Samuel I. A. Cohen, Michele Vendruscolo, Christopher M. Dobson, and Tuomas P. J. Knowles[a)]
Department of Chemistry, University of Cambridge, Lensfield Road, Cambridge CB2 1EW, United Kingdom

(Received 10 October 2010; accepted 16 June 2011; published online 12 August 2011)

Nucleated polymerisation processes are involved in many growth phenomena in nature, including the formation of cytoskeletal filaments and the assembly of sickle hemoglobin and amyloid fibrils. Closed form rate equations have, however, been challenging to derive for these growth phenomena in cases where secondary nucleation processes are active, a difficulty exemplified by the highly non-linear nature of the equation systems that describe monomer dependent secondary nucleation pathways. We explore here the use of fixed point analysis to provide self-consistent solutions to such growth problems. We present iterative solutions and discuss their convergence behaviour. We establish a range of closed form results for linear growth processes, including the scaling behaviours of the maximum growth rate and of the reaction end-point. We further show that a self-consistent approach applied to the master equation of filamentous growth allows the determination of the evolution of the shape of the length distribution including the mean, the standard deviation, and the mode. Our results highlight the power of fixed-point approaches in finding closed form self-consistent solutions to growth problems characterised by the highly non-linear master equations. © *2011 American Institute of Physics*. [doi:10.1063/1.3608917]

I. INTRODUCTION

There has been recently considerable renewed interest in the development of theoretical models that describe the general problem of growth of filamentous protein structures.[1–7] The theoretical analysis of such polymerising protein systems was initiated in the 1960s in the context of a range of functional biological assembly phenomena,[8–12] including the growth of actin and tubulin filaments. Furthermore, much experimental and theoretical attention has been focused on aberrant biological assembly, starting with sickle hemoglobin assembly,[13–16] and more recently the processes leading to the formation of amyloid fibrils often observed in association with neurodegenerative and other diseases.[17–24] In the overall kinetics of growth, secondary nucleation processes, including filament fragmentation, have emerged as dominant factors for amyloid formation[1,3,25–27] and prion assembly.[1,28,29] Such secondary events lead to a description of the growth problem through kinetic equations that are commonly highly non-linear, Fig. 1.

In order to address the difficulty in obtaining analytical results for the full time course of the reaction, we proposed[30,31] a self-consistent analysis scheme and showed that this approach yields closed form solutions to the growth problem. The focus of the present paper is to extend this approach to highly non-linear master equations by exploring the nature of the higher order solutions that emerge from the repeated application of the fixed-point iteration to the moment equations (Secs. II–VI) and also by exploring self-consistent solutions to the full filament length distribution (Sec. VII). We show that closed form solutions of high accuracy can be generated using this approach. In particular, we derive analytical results, valid for the full duration of the reaction, which describe in closed form the time evolution of the lower principal moments of filament systems that grow through primary nucleation, filament elongation, and either monomer independent or monomer dependent secondary nucleation. These higher order iterations also allow access to important corrections to the scaling laws that emerge from the analysis of the lower order solutions, as well as to information on the shape of the filament length distribution.

The differential equations that describe monomer-dependent secondary pathways involve very strong non-linearities in addition to those originating from the primary nucleation. These types of equations are not readily amenable to perturbative treatments as all of the non-linear terms contribute significantly to the overall reaction as shown in Fig. 2. The main result of this paper is an approach to treat such highly non-linear growth problems, and we provide an iterative scheme to obtain a closed form expression of high accuracy for the integrated rate laws (cf. Appendix B), the accuracy of which is illustrated in Fig. 2.

II. SECOND ORDER SELF-CONSISTENT SOLUTIONS

In the first part of this paper, we focus on higher order iterative solutions for the case where the secondary pathway is filament fragmentation and is hence monomer independent. This type of secondary pathway does not introduce non-linear

a)Author to whom correspondence should be addressed. Electronic mail: tpjk2@cam.ac.uk.

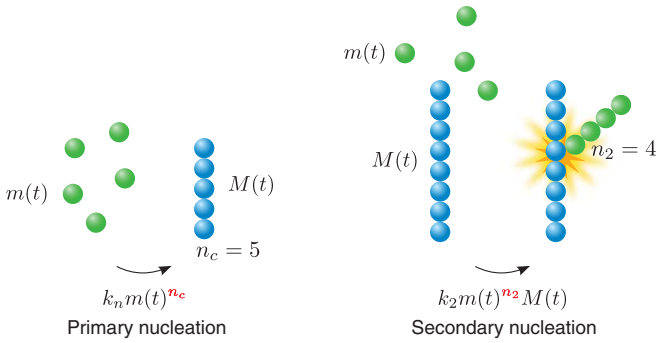

FIG. 1. Highly non-linear processes in protein polymerisation. The primary nucleation rate depends on the monomer concentration $m(t)$ with a power of the critical nucleus size n_c, and secondary nucleation processes depend on both the polymer concentration $M(t)$ and the monomer concentration to a power n_2; values of n_2 up to $n_2 = 30$ have been reported.[14,16] The special case of filament fragmentation (see Ref. 1) is monomer independent $n_2 = 0$.

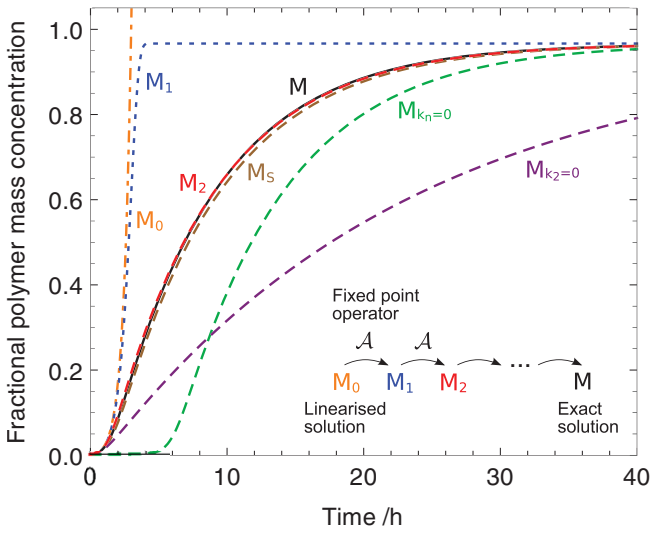

FIG. 2. Illustration of the nature of the solutions to highly non-linear growth problems derived using the fixed point scheme (insert). An analytical solution to filament growth through primary nucleation, monomer dependent secondary nucleation, filament elongation, and depolymerization [Eqs. (35) and (36)] is shown in red and the complete closed form self-consistent solution is provided in Appendix B, Eq. (B1). The brown dashed line is a simplified self-consistent solution also derived in this paper, Eq. (54). The black line is the exact numerical result. For comparison, the green dashed line is the numerical result neglecting primary nucleation, the purple dashed line is the numerical result neglecting secondary nucleation. The blue dotted line is the first order result (see Ref. 31) and the orange dotted-dashed line is the linearized solution (see Refs. 16, 32, 33, and 5). The parameters are: $n_c = 35$, $n_2 = 20$, $k_+ = 5 \times 10^4$ M^{-1} s^{-1}, $k_{\text{off}} = k_+ m_{\text{tot}}/30$, $k_2 m_{\text{tot}}^{n_2} = 5 \times 10^{-8}$ s^{-1}, $k_n m_{\text{tot}}^{n_c-1} = 5 \times 10^{-10}$ s^{-1}, $m_{\text{tot}} = 5 \times 10^{-5}$ M, $M(0) = 5 \times 10^{-11}$ M, $P(0) = M(0)/5000$.

terms into the equations for the principal moments, Eqs. (1) and (2), and therefore the only source of non-linearity is the elongation process [terms proportional to $M(t)P(t)$] and the primary nucleation process [terms proportional to a polynomial of degree n_c in $M(t)$].[31] The evolution of the principal moments, the polymer number concentration $P(t)$ and the polymer mass concentration $M(t)$, has been shown to obey the differential equations[5,9,29,34]

$$\frac{dP(t)}{dt} = k_-[M(t) - (2n_c - 1)P(t)] + k_n m(t)^{n_c}, \quad (1)$$

$$\frac{dM(t)}{dt} = 2\left[m(t)k_+ - k_{\text{off}} - \frac{k_- n_c(n_c-1)}{2}\right]P(t) + n_c k_n m(t)^{n_c}, \quad (2)$$

where $m(t) = m_{\text{tot}} - M(t)$ is the free monomer concentration and k_+, k_{off}, k_-, and k_n are the rate constants for elongation, depolymerisation, fragmentation, and primary nucleation, respectively. In order to recover the detailed scaling exhibited by solutions to the problem of filament growth under conditions where filament fragmentation enhances the number of free filament ends, we require self-consistent solutions that go beyond those previously obtained as the first order corrections restoring mass conservation[30,31] to the linearized solutions[5,16,32,33] which do not include mass conservation. We base our discussion on a fixed-point analysis; the kinetic problem is reformulated as a fixed-point equation[31] and subsequent applications of the fixed-point operator yield increasingly accurate iterative self-consistent solutions. The first improvement beyond the lowest order result[30,31] is obtained by establishing the second order self-consistent solution to the filament growth problem.

The self-consistent result obtained after one iteration has been shown to emerge as the simple closed form expression[31] for the polymer mass concentration

$$M_1(t) = M(\infty)[1 - \exp(-C_+ e^{\kappa t} + C_- e^{-\kappa t} + D)], \quad (3)$$

where the filament multiplication rate is defined as $\kappa = \sqrt{2[m(0)k_+ - k_{\text{off}}]k_-}$ for initial monomer concentration

TABLE I. Comparison of the first and second order self-consistent solutions for irreversible filament growth with fragmentation with exact results calculated numerically.

	First order	Second order	Exact
Polymer mass $\frac{M(t)}{M(\infty)} =$	$1 - \exp\left(-C_+ e^{-\kappa t} + C_- e^{-\kappa t} + \frac{\lambda^2}{\kappa^2}\right)$	$1 - \exp\left(\sum_{p=1}^{\infty}\left[\frac{(-C_+)^p}{p^2 p!}\left(e^{p\kappa t} - \sum_{q=0}^{2p-2}\frac{(p\kappa t)^q}{q!}\right) + \frac{C_-^p}{p^2 p!}\left(e^{-p\kappa t} - \sum_{q=0}^{2p-2}\frac{(-p\kappa t)^q}{q!}\right)\right] - \frac{M(0)}{M(\infty)}\right)$	
	$\kappa = \sqrt{2m(0)k_+k_-}$ $\lambda = \sqrt{2m(0)^{n_c}k_+k_n}$	$C_\pm = \frac{k_+P(0)}{\kappa} \pm \frac{M(0)}{2m(0)} \pm \frac{\lambda^2}{2\kappa^2}$	
Lag time $\tau_{\text{lag}} =$	$[\log(1/C_+) - 1.718]\kappa^{-1}$	$[\log(1/C_+) - 1.805]\kappa^{-1}$	$[\log(1/C_+) - 1.825]\kappa^{-1}$[a]
Maximal growth rate $r_{\max}/M(\infty) =$	$0.3679\,\kappa$	$0.3267\,\kappa$	$0.3182\,\kappa$[a]
No breakage limit $\frac{M(t)}{m_{\text{tot}}} \approx$	$1 - \exp\left(-t^2 k_+ k_n m_{\text{tot}}^{n_c}\right)$	$1 - \exp\left(-t^2 k_+ k_n m_{\text{tot}}^{n_c} + \frac{1}{6}t^4 k_+^2 k_n^2 m_{\text{tot}}^{2n_c} + \mathcal{O}(t^6)\right)$	$1 - \exp\left(-t^2 k_+ k_n m_{\text{tot}}^{n_c} + \frac{1}{6}t^4 k_+^2 k_n^2 m_{\text{tot}}^{2n_c} + \mathcal{O}(t^6)\right)$[b]
(no seeding $M(0) = 0$)			

[a]Numerical (Ref. 37).
[b]Equation (24).

$m(0)$, and the final polymer mass concentration[31,35] $M(\infty) \approx [2k_+m_{\text{tot}} - 2k_{\text{off}} - n_c(n_c-1)k_-]/(2k_+)$. The constants are functions of the initial conditions and of the rate constants k_n, k_+, k_{off}, and k_-

$$C_\pm = \frac{k_+P(0)}{\kappa} \pm \frac{k_+M(0)}{2[m(0)k_+ - k_{\text{off}}]} \pm \frac{\lambda^2}{2\kappa^2}, \tag{4}$$

$$D = \frac{\lambda^2}{\kappa^2} - \frac{M(0)}{M(\infty)} + \frac{k_+M(0)}{m(0)k_+ - k_{\text{off}}}, \tag{5}$$

where $\lambda = \sqrt{2k_+k_nm(0)^{n_c}}$ is the effective rate constant derived by Oosawa[8,9,31] for nucleated polymerization without secondary pathways. The aim of the present section of this paper is to generalise Eq. (3) to higher order approximations and recover the corresponding corrections to the scaling behaviour in the system kinetics. The two components of the fixed-point operator,[31] appropriate for this system, are derived by integration of Eqs. (1) and (2) to yield [30,31]

$$M(t) = M(\infty)(1 - e^{-\frac{M(0)}{M(\infty)} - 2k_+\int_0^t P(\tau)d\tau}), \tag{6}$$

$$P(t) = k_-e^{-(2n_c-1)k_-t}\left(P(0) + \int_0^t e^{(2n_c-1)k_-\tau}M(\tau)d\tau\right). \tag{7}$$

The convergence of the fixed-point scheme is most effective when the operator acts on a solution which is close to the final fixed point. In our first order solutions, this condition is better satisfied for early times, and therefore the accuracy of the first order self-consistent solution is less good for times corresponding to the reaction end point. The accuracy of the expression for $M(t)$ in Eq. (3) may be improved with higher order corrections from further fixed point iterations. This improvement corresponds to substituting the first order expression $P_1(t)$ into the integral operator for $M(t)$ in Eq. (6) to find a more accurate solution in this self-consistent scheme.

By substituting Eq. (3) into Eq. (7), the first order result for $P_1(t)$ has been shown to obey[31]

$$P_1(t) = k_-e^{-(2n_c-1)k_-t}\left\{P(0) + \int_0^t e^{(2n_c-1)k_-\tau}M(\infty) \times[1 - \exp(-C_+e^{\kappa\tau} + C_-e^{-\kappa\tau} + D)]d\tau\right\}. \tag{8}$$

For sufficiently large breakage rates ($C_+C_- \ll 1$) and at early times ($t \ll \kappa^{-1}$), the exponential term may be approximated as

$$\exp(-C_+e^{\kappa\tau} + C_-e^{-\kappa\tau} + D) \approx \exp(-C_+e^{\kappa\tau}) + \exp(C_-e^{-\kappa\tau}) - 1. \tag{9}$$

On rearrangement and expansion for early times $t \ll \kappa^{-1} \ll k_-^{-1}$, the integral Eq. (8) has a closed form expression valid for early times

$$P_1^e(t) = e^{-(2n_c-1)k_-t}\left(P(0) + \frac{k_-M(\infty)}{\kappa}[E_1(C_+e^{\kappa t}) - E_1(C_+) - E_1(-C_-e^{-\kappa t}) + E_1(-C_-) + 2\kappa t]\right). \tag{10}$$

where the exponential integral $E_1(t) = -Ei(-t) = \int_t^\infty e^{-s}/s\,ds$.

This result is accurate for significantly longer times than the linearized solution[31,32] used to generate $M_1(t)$ and would, therefore, be expected to produce an improved expression for $M(t)$ when operated on by Eq. (6). Indeed the correction for the first moment can now be obtained from Eq. (10) and Eq. (6) as $M_2(t)$. In this case, we obtain

$$\frac{M_2(t)}{M(\infty)} = 1 - \exp\left(-2k_+\int_0^t \mathcal{O}(k_-t)^2 + \frac{k_-M(\infty)}{\kappa}[E_1(C_+e^{\kappa t}) - E_1(C_+) + \kappa t] - \frac{k_-M(\infty)}{\kappa}[E_1(-C_-e^{-\kappa t}) - E_1(-C_-) - \kappa t]dt - \frac{M(0)}{M(\infty)}\right). \tag{11}$$

In order to carry out the integration in Eq. (11), the integrand is rewritten as

$$I = I_y + I_z = \frac{k_-M(\infty)}{\kappa}[\log(y) + E_1(C_+y) - E_1(C_+)] - \frac{k_-M(\infty)}{\kappa}[\log(z) + E_1(-C_-z) - E_1(-C_-)], \tag{12}$$

with $y = e^{\kappa t}$ and $z = e^{-\kappa t}$. The terms I_y and I_z may be integrated using an identical approach; we carry out the integration for I_y. Expansions around $y = 1$ ($t = 0$) yield

$$\log(y) = \sum_{p=1}^{\infty}(-1)^{p+1}\frac{(y-1)^p}{p}, \tag{13}$$

$$E_1(C_+y) - E_1(C_+) = \sum_{p=1}^{\infty}(-1)^p\frac{C_+^pE_{1-p}(C_+)(y-1)^p}{p!}, \tag{14}$$

and expanding the exponential integral about $C_+ = 0$ gives

$$E_{1-p}(C_+) = C_+^{-p}(p-1)! + \sum_{q=1}^{\infty}(-1)^q\frac{C_+^{q-1}}{(q-1)!(q-1+p)}. \tag{15}$$

Due to the convergence of the series, I_y may be obtained exactly

$$I_y = \frac{k_-M(\infty)}{\kappa}\sum_{p=1}^{\infty}\sum_{q=1}^{\infty}(-1)^{p+q}\frac{C_+^{p+q-1}(y-1)^p}{p!(q-1)!(q-1+p)}. \tag{16}$$

Transforming the rest of the integral into a function of the variable y, and writing $(y-1)^p$ as a binomial sum, the integration can be carried out exactly term by term. For small depolymerization rates,[31,36] $k_{\text{off}} \ll k_+m_{\text{tot}}$, this operation

results in

$$\int_0^t I_y dt \approx -\frac{1}{2k_+}\sum_{p=1}^{\infty}\sum_{q=1}^{\infty}(-1)^{p+q+1}C_+^{p+q-1}\frac{(-1)^p\kappa t + \sum_{r=0}^{p-1}(-1)^r\frac{p!}{r!(p-r)!(p-r)}(e^{(p-r)\kappa t}-1)}{p!(q-1)!(q-1+p)}. \quad (17)$$

The major contribution to the summation over r in Eq. (17) originates in the leading order exponentials where $r = 0$ and, similarly, for $C_+ \ll 1$ the leading order terms in the summation over q are given from $q = 1$, resulting in

$$\int_0^t I_y dt = -\frac{1}{2k_+}\sum_{p=1}^{\infty}(-C_+)^p\frac{(e^{p\kappa t}-1)}{p^2 p!}. \quad (18)$$

The result for I_z may be found through the replacement $C_+ \to -C_-$, yielding a compact result for $M_2(t)$

$$\frac{M_2(t)}{M(\infty)} = 1 - \exp\left(\sum_{p=1}^{\infty}\left[(-C_+)^p\frac{(e^{p\kappa t}-1)}{p^2 p!} + C_-^p\frac{(e^{-p\kappa t}-1)}{p^2 p!}\right] - \frac{M(0)}{M(\infty)}\right). \quad (19)$$

We now use this solution obtained in the early time limit $t \ll \kappa^{-1}$ and sufficiently large k_- ($C_-C_+ \ll 1$) to construct the full time-course solution. To this effect, we know the limit that should be obtained in the absence of fragmentation and depolymerisation (Oosawa limit,[9,31] Eq. (24)). Using this result to complete the missing terms in Eq. (19) by comparison with the special case,[9,31] Eq. (24), the full result for the second order iteration is obtained as

$$\frac{M_2(t)}{M(\infty)} = 1 - \exp\left(\sum_{p=1}^{\infty}\left[\frac{(-C_+)^p}{p^2 p!}\left(e^{p\kappa t} - \sum_{q=0}^{2p-2}\frac{(p\kappa t)^q}{q!}\right) + \frac{C_-^p}{p^2 p!}\left(e^{-p\kappa t} - \sum_{q=0}^{2p-2}\frac{(-p\kappa t)^q}{q!}\right)\right] - \frac{M(0)}{M(\infty)}\right). \quad (20)$$

This equation has an analogous form to the first order solution discussed in Refs. 30 and 31 but we note the presence of additional terms in the exponential. As in Part I,[31] a linear term $n_c k_n m_{\text{tot}}^{n_c-1} t$ has been neglected since the breakage rate is small such that most bonds in the system do not break over the reaction time.

Fig. 3 shows the first and second order iterations, given by Eqs. (3) and (20). From this figure, it is evident that the second order iteration offers a significant improvement in accuracy over the first order result in matching the exact solution and in particular offers significant improvement over the first order result towards the end of the growth phase.

In considering after how many terms the outer summation in Eq. (20) can be terminated whilst still offering a good approximation for $M(t)$, first note that the summation is absolutely convergent for any given t, with the absolute ratio between the $(p+1)$th and pth terms for long times $u_{p+1}/u_p = p^2(p+1)^{-3}C_+e^{\kappa t}$. The series converges in a small number of terms for times such that $C_+e^{\kappa t} \ll 1$, but for longer times

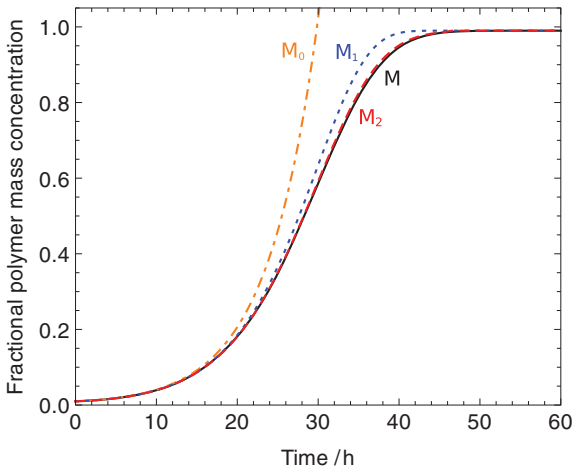

FIG. 3. Convergence of the first two fixed point analytical iterations towards the exact solution. The blue dotted line is the first order result, the red dashed line is the second order result, and the solid black line is the exact result. The orange dotted-dashed line is the early time limit linearized solution. The parameters are: $k_+ = 5 \times 10^4$ M^{-1} s^{-1}, $k_{\text{off}} = k_+ m_{\text{tot}}/100$, $k_- = 2 \times 10^{-8}$ s^{-1}, $k_n = 5 \times 10^{-5}$ M^{-1}s^{-1}, $m_{\text{tot}} = 1 \times 10^{-6}$ M, $n_c = 2$, $M(0) = 1 \times 10^{-8}$ M, $P(0) = M(0)/5000$. The summation in the second order iteration is truncated after 25 terms.

than this, a large number of terms is needed. Due to the alternating nature of the series, if the sum is terminated after an odd number of terms then in the limit $t \to \infty$ it will yield a large negative number, whereas for termination after an even number of terms the result gives a large positive number in this limit. Since the summation is within an exponential function in Eq. (20), when truncating after an odd number of terms the exponential term tends to zero and $M(t) \to M(\infty)$ in the long time limit, as required. Conversely, if the sum is terminated after an even number of terms then in the limit $t \to \infty$, $M(t) \to -\infty$. Hence, enough terms must be included before terminating the summation such that the ratio between the last included and first omitted term is small for times before which $M(t) \sim M(\infty)$, and the summation must also be terminated after an odd number of terms. Interestingly, the scaling behaviour of the system (Sec. VI) ensures that the number of required terms is approximately independent of the kinetic parameters.

Using the parameters of Fig. 3, these convergence conditions are fully satisfied terminating the summation after 25 terms. The result including just three terms, offering the first improvement over the first order iteration $M_1(t)$,[31] is given explicitly by

$$\frac{M_2(t)}{M(\infty)} = 1 - \exp\left(-(e^{\kappa t}-1)C_+ + (e^{-\kappa t}-1)C_- + (e^{2\kappa t}-1-\pi_+^{(2)}(t))\frac{C_+^2}{8} + (e^{-2\kappa t}-1-\pi_-^{(2)}(t))\frac{C_-^2}{8} - (e^{3\kappa t}-1-\pi_+^{(3)}(t))\frac{C_+^3}{54} + (e^{-3\kappa t}-1-\pi_-^{(3)}(t))\frac{C_-^3}{54} - \frac{M(0)}{M(\infty)}\right), \quad (21)$$

where $\pi_\pm^{(2)}(t) = \pm 2\kappa t + 2\kappa^2 t^2$, $\pi^{(3)}(t) = \pm 3\kappa t + 9\kappa^2 t^2/2 \pm 9\kappa^3 t^3/2 + 27\kappa^4 t^4/8$. We note that compared with

the first order result $M_1(t) = M(\infty)[1 - \exp(-C_+(e^{\kappa t} - 1) + C_-(e^{-\kappa t} - 1) - M(0)/M(\infty))]$ there are new terms $\sim e^{2\kappa t}, e^{3\kappa t}$ and associated polynomials in κt in the exponent.

III. INFRANGIBLE FILAMENTS

For a system of infrangible filaments, $k_- = 0$, undergoing irreversible growth, $k_{\text{off}} = 0$, in the absence of pre-formed seed material, $M(0) = P(0) = 0$, the limit of Eq. (20) is given as

$$\frac{M_2(t)}{m_{\text{tot}}} = 1 - \exp\left(\sum_{p=1}^{\infty} \frac{(-1)^p}{p^2 p!} \frac{2\,(k_n k_+ {m_{\text{tot}}}^{n_c})^{\,p}}{(2p)!} (pt)^{2p}\right), \tag{22}$$

where the first few terms are given by

$$\frac{M_2(t)}{m_{\text{tot}}} = 1 - \exp\Big(- t^2 k_+ k_n m_{\text{tot}}^{n_c} + \frac{1}{6} t^4 k_+^2 k_n^2 m_{\text{tot}}^{2n_c} - \frac{3}{80} t^6 k_+^3 k_n^3 m_{\text{tot}}^{3n_c} + \mathcal{O}(t^8)\Big). \tag{23}$$

In particular, higher powers of t are now present in comparison with the first order result.[31] It is interesting to note that the exact Oosawa result for irreversible growth of infrangible filaments[9] in the absence of seeds and depolymerisation, $M(t)/m_{\text{tot}} = 1 - \text{sech}^{2/n_c}(\sqrt{n_c k_n k_+ m_{\text{tot}}^{n_c}})$, admits the series expansion

$$\frac{M(t)}{m_{\text{tot}}} = 1 - \exp\Big(- t^2 k_+ k_n m_{\text{tot}}^{n_c} + \frac{1}{6} t^4 k_+^2 k_n^2 m_{\text{tot}}^{2n_c} - \frac{2}{45} t^6 k_+^3 k_n^3 m_{\text{tot}}^{3n_c} + \mathcal{O}(t^8)\Big). \tag{24}$$

It can be seen that whilst the first order result is correct to $\mathcal{O}(t^2)$,[31] the second order iteration now reproduces the correct limit to $\mathcal{O}(t^4)$. The limits given by the first and second order analytical results are compared with the exact result in Fig. 4, where the second order result is seen to provide a significant improvement.

In considering the limit $k_- \to 0$, we note that in the fixed-point analysis presented so far, the fixed-point operator neglects terms $\mathcal{O}(k_n)$. This is an accurate approximation for the first two self-consistent solutions in the case of fragmenting filaments which we have presented, since the influence of the primary nucleation comes mainly from its effect on the linear solutions used as the starting point of the fixed point scheme. Whilst the rate of creation of filaments from fragmentation increases as the reaction proceeds, the rate of creation of filaments from primary nucleation slows as monomer is depleted. Hence primary nucleation is most important for earlier times, and its relative importance compared to secondary nucleation decreases monotonically. Repeated iteration, however, using our fixed point scheme, would result in higher order solutions that ultimately converge towards the solution of the master equation neglecting $\mathcal{O}(k_n)$.

A strategy to ensure the correct convergence behaviour is to enforce the exact early time limit behaviour, including $\mathcal{O}(k_n)$, in each iteration, which is already satisfied in the first two iterations presented here. As a general procedure for higher iterations, the system can be evolved using the linearized early time solutions $M_0(t)$ and $P_0(t)$ derived in Part I,[31] which include $\mathcal{O}(k_n)$, for as long as the early time solution is a good approximation to the exact solution. If the time for which the early solution remains a good approximation is denoted by t_0, for times greater than t_0 the fixed point iteration scheme is then used to find $M(t)$, but now using $M_0(t_0)$, $P_0(t_0)$ from the early time solutions as the initial conditions. The final solution, which converges to the solution including $\mathcal{O}(k_n)$, is then given by the early time limit result continued piecewise to the higher order fixed point iteration at t_0.

For systems where the secondary pathway is monomer-dependent (Sec. V), the relative importance of primary and secondary nucleation will no longer, in general, vary monotonically as the reaction proceeds, and so the explicit inclusion of terms $\mathcal{O}(k_n)$ in higher iterations, including the second-order result, is then required.

IV. CORRECTIONS TO LOWER ORDER SCALING LAWS

The availability of a highly accurate analytical solution to the growth kinetics over the full time course of the polymerisation reaction provides us with the opportunity to analyse the corrections to the scaling behaviour in the lag time that has emerged from the lower order solutions.[30–32] In this section, we show that the numerical values of the coefficients in the scaling laws from the first order solutions are significantly improved when considering the corrections obtained from the second order results, Table I. We recall that the lag time, τ_{lag}, is defined in terms of the maximum growth rate, r_{max}, and the time at which the maximum growth rate occurs, t_{max}

$$\tau_{\text{lag}} = t_{\text{max}} - \frac{M(t_{\text{max}})}{r_{\text{max}}}. \tag{25}$$

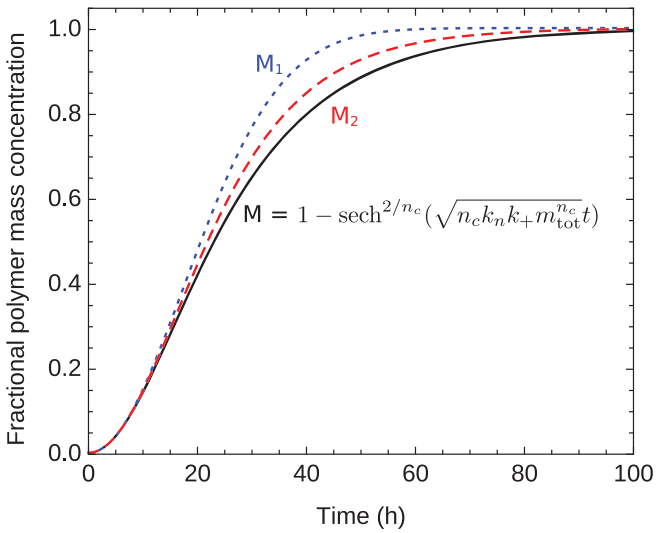

FIG. 4. Convergence of the first two fixed-point analytical iterations towards the exact solution (Refs. 8 and 9) in the absence of breakage. The blue dotted line is the first order result, the red dashed line is the second order result, and the solid black line is the numerical result. The parameters are: $k_+ = 5 \times 10^4$ M^{-1} s^{-1}, $k_{\text{off}} = k_- = 0$ s^{-1}, $k_n = 5 \times 10^{-4}$ $\text{M}^{-1}\text{s}^{-1}$, $m_{\text{tot}} = 5 \times 10^{-6}$ M, $n_c = 2$, $M(0) = P(0) = 0$.

In order to obtain the expressions for $t_{\max}$, $r_{\max}$, and $M(t_{\max})$ we first perform a substitution to introduce the dimensionless quantity $y = C_+ e^{\kappa t}$ into the long-time limit, $t \gg \kappa^{-1}$, of Eq. (20)

$$\frac{M_2(t)}{M(\infty)} = 1 - \exp\left(\sum_{p=1}^{\infty}(-C_+)^p \frac{e^{p\kappa t}}{p^2 p!}\right), \tag{26}$$

such that the value of y that occurs when $t = t_{\max}$ is $y_{\max} = C_+ e^{\kappa t_{\max}}$ whereby the explicit dependencies on C_+ and κ have been subsumed into the change of variable. Explicitly, $t_{\max}$ is given by

$$t_{\max} = \frac{\log\left(\frac{y_{\max}}{C_+}\right)}{\kappa} = \frac{\log(1/C_+) + \log(y_{\max})}{\kappa}. \tag{27}$$

Remarkably, this form maintains the inverse correlation between the multiplication rate κ and the lag time,[30,31] but introduces a correction to the proportionality constant. Note that $y_{\max} = 1$ recovers the result obtained from the first iteration.[31]

The determination of $y_{\max}$ requires the evaluation of the inflection point of $M_2(t)$. Under the substitution $dy/dt = \kappa y$, the inflection point is found as

$$\left(\frac{d^2 M_2}{dy^2} + \frac{1}{y}\frac{dM_2}{dy}\right)_{y=y_{\max}} = 0. \tag{28}$$

which is a polynomial equation for $y_{\max}$

$$0 = \left(\sum_{q=1}^{\infty}\frac{(-1)^q y_{\max}^{q-1}}{qq!}\right)^2 + \sum_{q=1}^{\infty}\frac{(-1)^q y_{\max}^{q-2}}{q!}. \tag{29}$$

This equation must be solved numerically and results in $y_{\max} = 0.99616$. This value determines the maximum growth rate, $r_{\max} = (dM/dt)_{t=t_{\max}} = \kappa y (dM/dy)_{y=y_{max}}$, as

$$r_{\max} = 0.3267\, M(\infty)\kappa, \tag{30}$$

which may be compared with the first order and exact numerical results to show a significant improvement over the first order

$$r_{\max} = \begin{cases} 0.3679\, M(\infty)\kappa & \text{first iteration} \\ 0.3267\, M(\infty)\kappa & \text{second iteration} \\ 0.3182\, M(\infty)\kappa & \text{exact numerical} \end{cases}. \tag{31}$$

Substituting $y_{\max}$ into Eq. (25) yields the lag time scaling $\tau_{\text{lag}} = [\log(1/C_+) + s]\kappa^{-1}$ for $s = \log(y_{\max}) - \kappa M(t_{\max})/r_{\max}$, resulting in

$$s = \log(y_{\max}) + \frac{1 - \exp\left(\sum_{p=1}^{\infty}\frac{(-1)^p y_{\max}^p}{p^2 p!}\right)}{\left(\sum_{p=1}^{\infty}\frac{(-1)^p y_{\max}^p}{pp!}\right)\exp\left(\sum_{p=1}^{\infty}\frac{(-1)^p y_{\max}^p}{p^2 p!}\right)} = -1.8053. \tag{32}$$

Therefore

$$\tau_{\text{lag}} = \left[\log(1/C_+) - 1.805\right]\kappa^{-1}. \tag{33}$$

As a consistency check we can verify that setting the upper limits of the summations to unity and setting $y_{\max} = 1$ recovers $s = -e + 1 \approx -1.718$, which is the first iteration result,[31] as expected. Summarising the three results

$$\tau_{\text{lag}} = \begin{cases} \left[\log(1/C_+) - 1.718\right]\kappa^{-1} & \text{first iteration} \\ \left[\log(1/C_+) - 1.805\right]\kappa^{-1} & \text{second iteration} \\ \left[\log(1/C_+) - 1.825\right]\kappa^{-1} & \text{exact numerical} \end{cases} \tag{34}$$

The second order result is a substantial improvement over the first, with the numerical constant now correct to within 1% of the exact result.

V. MONOMER DEPENDENT SECONDARY NUCLEATION

In the second part of this paper, we focus on polymerisation processes where the secondary pathway is concentration dependent.[4,32] The analysis of this type of growth process was pioneered by Eaton and Ferrone[16,32] in their work on sickle hemoglobin gelation. Linear solutions can be obtained much in the same way as for fragmentation but this type of process introduces highly non-linear terms into the master equations which become relevant when mass conservation is enforced. Consequently, such processes are more challenging to treat than the fragmentation case, and we anticipate less rapid convergence of the fixed point scheme. In addition, since the secondary nucleation term is now also affected by the monomer depletion, the relative importance of the primary and secondary nucleation may vary in a more complicated way than in the fragmentation case where the relative importance of primary to secondary nucleation decreases monotonically as the reaction proceeds. Hence, in the case of monomer-dependent secondary nucleation, the inclusion of primary nucleation only in the early time limit is expected to be insufficient in describing accurately the full time course of the reaction.

For the case of monomer dependent secondary nucleation, the equations for the moments become[4,16,32]

$$\frac{dP(t)}{dt} = k_2 M(t) m(t)^{n_2} + k_n m(t)^{n_c}, \tag{35}$$

$$\frac{dM(t)}{dt} = 2(m(t)k_+ - k_{\text{off}})P(t) + n_c k_n m(t)^{n_c} + n_2 k_2 M(t) m(t)^{n_2}, \tag{36}$$

where the rate of production of filaments through the secondary pathway, $k_2 M(t) m(t)^{n_2}$, has a monomer-dependence for $n_2 \geq 1$, with the special case $n_2 = 0$ recovering approximately the polymer mass concentration found in the case of fragmenting filaments.[31] Interestingly, the introduction of a monomer-dependence in the secondary pathway implies that there will be two distinct phases of behaviour. At early times, when the monomer is not heavily depleted, the behaviour of the system is analogous to a system of fragmenting filaments, leading to exponential type growth in both $P(t)$ and

$M(t)$, as can be seen from the linearized form $k_2 M(t) m(t)^{n_2} \approx k_2 M(t) m_{\text{tot}}^{n_2}$ that emerges when $m(t) \approx m_{\text{tot}}$. At later times, as the monomer becomes depleted, there will be an inflection point in $P(t)$ beyond which the growth is not of exponential type and instead approaches that of a primary nucleation dominated system described by Oosawa[8,9] with a modified nucleation rate. The latter identification can be made explicit by writing $k_2 M(t) m(t)^{n_2} = k_2 m(t)^{n_2} (m_{\text{tot}} - m(t)) \approx k_2 m(t)^{n_2} m_{\text{tot}}$, which emerges when $m(t) \ll m_{\text{tot}}$, leading to a contribution from secondary nucleation in Eq. (35) that is of equivalent form to the term describing primary nucleation. In the case of fragmenting filaments, only the exponential phase emerges over the timescale of the polymerisation reaction, resulting in that case in the expectation that early time linearized solutions could be extended in validity over the full time course using a small number of fixed point iterations (Ref. 31 and Sec. II). In the present case, however, we expect to have to account explicitly for both phases of behaviour in the proliferation of filaments in order to achieve rapid convergence.

The starting point for our analysis in this section is given by recalling the first-order self-consistent result[30,31] for the kinetics of this process that has been derived by extending the validity of the early-time linearized solutions[16,31] via a self-consistent fixed-point iteration[30,31]

$$M_1(t) \approx M(\infty)[1 - \exp(-C_+ e^{\kappa t} + C_- e^{-\kappa t} + D)], \quad (37)$$

for the polymer mass concentration M_1 with $\kappa = \sqrt{2m(0)^{n_2}[m(0)k_+ - k_{\text{off}}]k_2}$ and $C_\pm \approx k_+ P(0)/\kappa \pm k_+ M(0)/\{2[m(0)k_+ - k_{\text{off}}]\} \pm \lambda^2/(2\kappa^2)$, $D = \lambda^2/\kappa^2 - M(0)/M(\infty) + k_+ M(0)/[m(0)k_+ - k_{\text{off}}]$. The long-time limit is given by $M(\infty) \approx m_{\text{tot}} - k_{\text{off}}/k_+$. Crucially, we note that whilst this first order result is a significant improvement over the linear results known previously, it becomes increasingly inaccurate as n_2 is increased as shown in Fig. 2. The strategy for studying this system to a higher level of accuracy, and hence to find a more accurate solution, is to consider explicitly the two phases of behaviour discussed above. To carry out this programme in practice, we first perform a second order iteration based on the early time exponential input, following the fragmentation case, neglecting $\mathcal{O}(k_n)$. This result will be accurate for earlier times before the inflection point in $P(t)$, but would be expected to be less accurate for later times beyond this. The accuracy of the solution at later times can be improved by accounting for the deviation of $P(t)$ from exponential behaviour in the initial input for the fixed point scheme; as a general strategy we use the solution itself to provide a new linearization as an input for a subsequent fixed-point scheme that will be accurate at later times. An additional advantage of this two part approach is the possibility of including explicitly the primary nucleation terms in the fixed point operator for later times. The two solutions that emerge from this analysis, each requiring only a small number of terms to remain convergent over a smaller time range, can then be continued piecewise together at an appropriate time given in closed form where the transition between exponential type and Oosawa type behaviour occurs; in this paper we make the natural choice of the point of inflection of $P(t)$ for this purpose.

Finally, through studying the two types of behaviour present in this system, we are able to construct a single elementary expression which is able to account accurately for both the exponential and Oosawa type growth phases. To this effect, we develop a simple closed form analytical result, Eq. (54), to Eqs. (35) and (36) that has intermediate accuracy between the first order results[31] and the highly accurate second order results also presented here.

A. Exponential type growth prior to the inflection point

In analogy with the treatment of fragmenting filaments, the second order solution in the presence of secondary nucleation can be obtained in our fixed point scheme as

$$M(t) = M(\infty)\left[1 - \exp\left(-\frac{M(0)}{M(\infty)} - 2k_+ \int_0^t P(\tau) d\tau\right)\right]. \quad (38)$$

Following our analysis of a system of frangible filaments, we first derive a result for $P_1(t)$ for early times. To obtain the first iteration result for $P(t)$, we substitute Eq. (37) into Eq. (35). Neglecting terms $\mathcal{O}(k_n)$, the equation to be solved for $P_1(t)$ becomes

$$\frac{dP_1^e(t)}{dt} = k_2 M_1(t) m_1(t)^{n_2}. \quad (39)$$

Conservation of mass, $M_1(t) = m_{\text{tot}} - m_1(t)$, results in

$$\frac{dP_1^e(t)}{dt} = k_2 m_{\text{tot}} m_1(t)^{n_2} - k_2 m_1(t)^{n_2+1}, \quad (40)$$

where the monomer concentration $m_1(t) \approx m(0) \times \exp(-C_+ e^{\kappa t} + C_- e^{-\kappa t} + D)$ is given for small depolymerisation rates from Eq. (37). Performing an equivalent approximation to that of Eq. (9) results in the expression

$$\frac{dP_1^e(t)}{dt} \approx k_2 m(0)^{n_2+1}[\exp(-n_2 C_+ e^{\kappa t}) - \exp(n_2 C_- e^{-\kappa t}) - \exp(-(n_2+1) C_+ e^{\kappa t}) + \exp((n_2+1) C_- e^{-\kappa t})]. \quad (41)$$

Integrating both sides with respect to time yields the self-consistent solution for the polymer number concentration

$$P_1^e(t) = P(0) + \frac{k_2 m(0)^{n_2+1}}{\kappa}[E_1((n_2+1)C_+ e^{\kappa t}) - E_1((n_2+1)C_+) - E_1(-(n_2+1)C_- e^{-\kappa t}) + E_1(-(n_2+1)C_-) - E_1(n_2 C_+ e^{\kappa t}) + E_1(n_2 C_+) + E_1(-n_2 C_- e^{-\kappa t}) - E_1(-n_2 C_-)], \quad (42)$$

which is analogous to Eq. (10) from our treatment of fragmenting filaments.

We substitute $y = e^{\kappa t}$, $z = e^{-\kappa t}$ into Eq. (42) so that the integrand from Eq. (38) can be written as the difference between two integrands of identical form as in the case of

fragmenting filaments, Eq. (12). Thus, the solution is given by the difference between these two known results Eq. (18). Making the same asymptotic analysis as for frangible filaments, Eq. (20), gives the closed form expression

$$\frac{M_2^{\text{series}}(t)}{M(\infty)} = 1 - \exp\left(\sum_{p=1}^{\infty}\left[\frac{(-C_+)^p((1+n_2)^p - n_2^p)}{p^2 p!}\right.\right.$$
$$\times\left(e^{p\kappa t} - \sum_{q=0}^{2p}\frac{(p\kappa t)^q}{q!}\right) + \frac{C_-^p((1+n_2)^p - n_2^p)}{p^2 p!}$$
$$\times\left(e^{-p\kappa t} - \sum_{q=0}^{2p}\frac{(-p\kappa t)^q}{q!}\right) + \frac{(-C_+)^p}{p^2 p!}$$
$$\times\left(\frac{(p\kappa t)^{2p-1}}{(2p-1)!} + \frac{(p\kappa t)^{2p}}{(2p)!}\right) + \frac{C_-^p}{p^2 p!}$$
$$\left.\left.\times\left(\frac{(-p\kappa t)^{2p-1}}{(2p-1)!} + \frac{(-p\kappa t)^{2p}}{(2p)!}\right)\right] - \frac{M(0)}{M(\infty)}\right. \tag{43}$$

This equation, which is accurate for early times, in particular before the inflection point in $P(t)$, has an analogous form to the result obtained for frangible filaments, Eq. (20), except for the presence of the multiplying factor $(1+n_2)^p - n_2^p$ in each term and additional polynomial terms. Furthermore, as expected, Eq. (43) reduces to Eq. (20) for $n_2 = 0$.[31]

The convergence discussion from the fragmenting growth section applies to this result as well, except that here the additional multiplicative factor, which increases exponentially with the index of summation, will reduce the convergence rate of the series. Specifically, the rate of convergence in Eq. (43), for the same timescale, is approximately a factor of $(1+n_2)$ slower than that observed for the analogous series in the fragmentation case. Crucially, however, whilst the first order iteration results, Eqs. (3) and (37), predict a similar timescale for the completion of the reaction both for the fragmentation and monomer-dependent secondary nucleation cases, the more accurate second order iteration result, Eq. (43), shows that the kinetic profile in the latter case is extended in time, with the end point being severely underestimated by the first iteration. This behavior originates from the transition from the exponential type growth in fibril number, which is observed throughout the time course for fragmenting filaments, to a slower growth form. A consequence of this observation is that the truncation of the summation must be valid in the monomer dependent secondary nucleation case over a much longer timescale than analogous curves in the fragmentation case. Hence, although only $(1+n_2)$ times more terms are required to give convergence over the same timescale, many more terms are required to provide a valid truncation over the extended timescale present in the monomer-dependent case. In the present solution scheme, the requirement for large numbers of terms in Eq. (43) is never realised, since the solution Eq. (43) will only be utilised up to the inflection point in $P(t)$, such that typically only terms up to $p = 3$ are required in the summation.

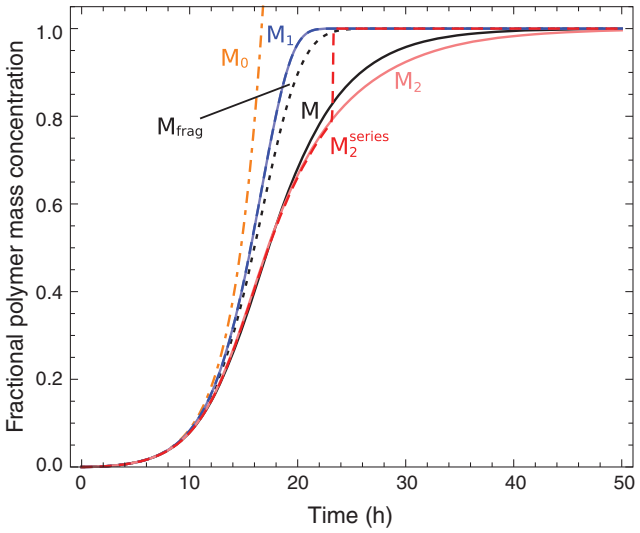

FIG. 5. Convergence of the nth fixed point iteration, $M_n(t)$, using the early time linearization. M_1 (blue dashed, Eq. (3)), M_2^{series} (red dashed, Eq. (43) with 75 terms), exact solution including $\mathcal{O}(k_n)$ (black). The lighter solid lines show the corresponding numerical results. The black dotted line is the exact result for the analogous fragmentation case for comparison. The orange dotted-dashed line is the early time linearization. The parameters are $M(0) = P(0) = 0M$, $k_+ = 5 \times 10^4$ M^{-1} s^{-1}, $k_{\text{off}} = 0$, $k_2 m(0)^{n_2} = 2 \times 10^{-8}$s^{-1}, $k_n = 2 \times 10^{-5}$ M^{-1}s^{-1}, $m_{\text{tot}} = 5 \times 10^{-6}$M, $n_c = 2$, $n_2 = 2$.

The convergence behaviour is demonstrated in Fig. 5, where the first two analytical iterations and the corresponding numerical results are shown. For comparison, we also consider the analogous fragmentation induced growth process obtained by identifying $k_- = k_2 m(0)^{n_2}$ and resulting in a secondary process which for $t = 0$ has the same effect as that of the monomer-dependent case. In this analogous fragmentation case, 25 terms in the summation are sufficient to prevent any significant errors from being introduced in to the summation; this success is due to the fact that the divergence in the series occurs after the reaction end-point when $M(t) \approx m_{\text{tot}}$ and is therefore inconsequential to the description of the growth phenomenon. In agreement with the convergence discussion above, it is observed in Fig. 5 that with $n_2 + 1 = 3$ times as many terms, i.e. 75, the summation from Eq. (43) is valid to the same time in the monomer dependent secondary nucleation case as in the fragmentation case, as shown by the fact that the step indicating the divergence in the series Eq. (43) (red dashed line) occurs precisely at the end-point of the fragmentation case (black dotted line).

The change in the shape of the curve relative to the case of fragmenting filaments can also be seen in the scaling of the lag time. Although this has the same form as for frangible filaments, the constant term in the scaling law is changed, reflecting the change in the shape of the kinetic profile. The scaling law from the second iteration result can be found using the same approach as in the fragmentation case, and the results for different vales of n_2 are shown

below

$$\tau_{\text{lag}}=\begin{cases}\left[\log(1/C_+)-1.718\right]\kappa^{-1} & \text{first iteration, all } n_2\\ \left[\log(1/C_+)-1.805\right]\kappa^{-1} & \text{second iteration, } n_2=0\\ \left[\log(1/C_+)-2.023\right]\kappa^{-1} & \text{second iteration, } n_2=1\\ \left[\log(1/C_+)-2.225\right]\kappa^{-1} & \text{second iteration, } n_2=2\\ \left[\log(1/C_+)-2.684\right]\kappa^{-1} & \text{second iteration, } n_2=5\\ \left[\log(1/C_+)-3.167\right]\kappa^{-1} & \text{second iteration, } n_2=10\end{cases}. \tag{44}$$

As expected, $n_2=0$ recovers the scaling characteristic of the growth of fragmenting filaments. As n_2 is increased, the first iteration result becomes increasingly poor. In particular, the end time is increasingly underestimated for increasing n_2, and so more and more terms are needed in the summation for the second order iteration using Eq. (43).

We note that the integrand that emerges from substituting Eq. (42) into Eq. (38) may also be integrated by re-writing

$$\begin{aligned}I=&\frac{k_2m(0)^{n_2+1}}{\kappa}[g_+(n_2+1)-g_+(n_2)\\&-g_-(n_2+1)+g_-(n_2)\\&+E_1(n_2C_+)-E_1((n_2+1)C_+)\\&-E_1(-n_2C_-)+E_1(-(n_2+1)C_-)],\end{aligned} \tag{45}$$

with the functions $g_+(x)=E_1(xC_+e^{\kappa t})$ and $g_-(x)=E_1(-xC_-e^{-\kappa t})$. Since the integrand contains the same functions $g_\pm$ evaluated with different arguments, the integrand can be rewritten exactly as

$$\begin{aligned}I=&\frac{k_2m(0)^{n_2+1}}{\kappa}\left(\sum_{i=1}^{\infty}\frac{1}{i!}\frac{d^ig_+(x)}{dx^i}\bigg|_{x=n_2}-\sum_{i=1}^{\infty}\frac{1}{i!}\frac{d^ig_-(x)}{dx^i}\bigg|_{x=n_2}\right.\\&+E_1(n_2C_+)-E_1((n_2+1)C_+)-E_1(-n_2C_-)\\&\left.+E_1(-(n_2+1)C_-)\right).\end{aligned} \tag{46}$$

This expression can be evaluated and integrated analytically term by term. For $n_2\geq 2$, an expansion to the fifth derivative is sufficient to give an excellent approximation to the exact result of the integral, with the result becoming more accurate as n_2 increases.

B. Oosawa type growth post-inflection point

The result Eq. (43) is accurate for all initial conditions and early and intermediate times and gives in closed form the time evolution of a filamentous system that grows through monomer dependent secondary nucleation and filament elongation. In order to extend the applicability of the solution to later times, we will use Eq. (43) to provide the appropriate initial conditions at the characteristic inflection point in the sigmoidal growth curve for the polymer number concentration to initiate a new fixed point iteration providing a more accurate description past the inflection point. This new linearization will account for the change in form of the increase in polymer number that emerges at later times in the reaction. Crucially, this approach will also enable us to include exactly the primary nucleation terms into the fixed-point operator, which is vital as the relative balance of primary and secondary nucleation varies as the reaction proceeds.

We consider as the initial input to the late-time fixed point scheme the straight line $P_0^{t_{\text{maxP}}}(t)$ that matches $P(t)$ and its gradient at its point of inflection in the reaction profile; the time corresponding to the inflection point is denoted by t_{maxP}. The linear input is expected to account better for the Oosawa type growth phase than the early time exponential input that is used prior to the inflection point. The choice for the separation between the early and late time solutions is made since beyond the inflection point in $P(t)$, the functional form of $P(t)$ is clearly not well described by exponential growth. In addition, at the point of inflection the second derivative of $P(t)$ is zero and therefore a linear approximation is valid here up to the third derivative. The concentration of free monomer $m_*=m(t_{\text{maxP}})$ at the time corresponding to the point of inflection is given through differentiation of Eq. (35) and enforcing the condition $d^2P/dt^2=0$ to yield

$$0=k_2n_2m_*^{n_2-1}m_{\text{tot}}-k_2(n_2+1)m_*^{n_2}+n_ck_nm_*^{n_c-1}. \tag{47}$$

First note that in the case $k_n=0$, Eq. (47) has the simple solution $m_*=m_{\text{tot}}n_2/(n_2+1)$ and to lowest order the nucleation terms can be included through the use of a Newton-Raphson correction to yield

$$m_*=\eta-\frac{k_n\eta^{n_c-1}n_c}{k_nn_c(n_c-1)\eta^{n_c-2}-k_2n_2\eta^{n_2-2}m_{\text{tot}}}, \tag{48}$$

where $\eta=m_{\text{tot}}n_2/(1+n_2)$. From the first order iteration result, Eq. (37), the time to reach m_* is given approximately by

$$t_{\text{maxP}}=\kappa^{-1}\log\left(\frac{-b+\sqrt{b^2+4C_+C_-}}{2C_+}\right), \tag{49}$$

for $b=\log(m_*/m(0))-D$ with m_* from Eq. (48) except for the special case $m_*>m(0)$ or $(1+n_2)k_2m(0)^{n_2-n_c}[m(0)-\eta]<n_ck_n$, corresponding to there being no (or two) points of inflection in P, for which we set $m_*=m(0)$ such that $t_{\text{maxP}}=0$.

Hence, our new initial linearization of $M(t)$ is given as

$$M_0^{t_{\text{maxP}}}(t)=\alpha+\beta(t-t_{\text{maxP}}), \tag{50}$$

with $\alpha=M_2(t_{\text{maxP}})$ and $\beta=\dot{M}_2(t_{\text{maxP}})$ where $M_2(t)$ is given by Eq. (43); as we only require the pre-inflection point solution Eq. (43) to be valid until t_{maxP}, typically only terms in the sum until $p=3$ are required for adequate convergence.

The corresponding initial solution for $P(t)$ may be found from the differential equations Eq. (35)

$$P_0^{t_{\text{maxP}}}(t)=\gamma+\delta(t-t_{\text{maxP}}), \tag{51}$$

with $\gamma\approx\dot{M}_2(t_{\text{maxP}})/[2(m_2(t_{\text{maxP}})k_+-k_{\text{off}})]$ and $\delta=k_2M_2(t_{\text{maxP}})m_2(t_{\text{maxP}})^{n_2}+k_nm_2(t_{\text{maxP}})^{n_c}$, and $m_2(t)=m_{\text{tot}}-M_2(t)$. Inserting Eq. (51) into Eq. (36), the first self-consistent solution for M is found by direct integration, neglecting direct consumption of monomer through the nucleation processes.

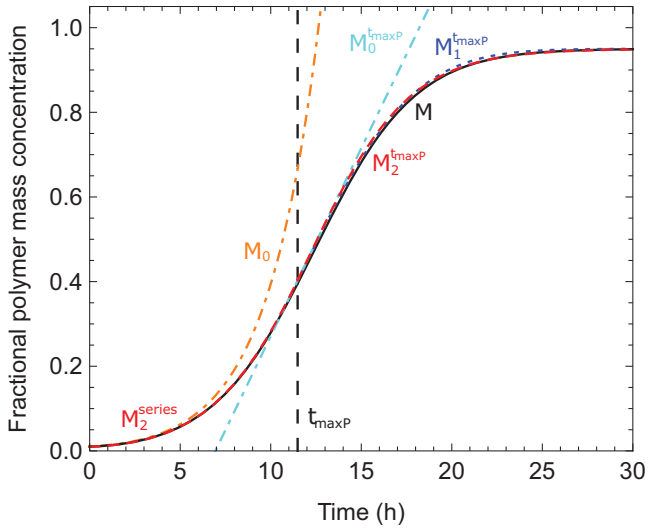

FIG. 6. The solution found using a second linearization about the point of inflection, t_{maxP} (indicated by the vertical black dotted line), is continued piecewise to M_2^{series}. For clarity we illustrate the case $n_2 = 1$, where $M(t_{maxP}) \sim m_{tot}/2$. The cyan dotted-dashed line is the new initial approximation, Eq. (50). For $t < t_{maxP}$, the red dashed line is M_2^{series} (Eq. (43) with 3 terms). For $t > t_{max}$, the blue dashed line is the first order iteration given by the new expression, $M_1^{t_{max}}$ (Eq. (52)), and the red dashed line is the corresponding second order iteration, $M_2^{t_{max}}$ (Eq. (A4)). The orange dotted-dashed line is the early time linearization. The parameters are $M(0) = 5 \times 10^{-8}$ M, $P(0) = M(0)/5000$, $k_+ = 2 \times 10^4$ M^{-1} s^{-1}, $k_{off} = k_+ m_{tot}/20$, $k_2 m_{tot}^{n_2} = 5 \times 10^{-8} s^{-1}$, $k_n = 1 \times 10^{-4}$ $M^{-1} s^{-1}$, $m_{tot} = 5 \times 10^{-6}$ M, $n_c = 2$, $n_2 = 1$.

With the condition $M(t_{maxP}) = \alpha$ we obtain

$$\frac{M_1^{t_{maxP}}(t)}{M(\infty)} = 1 - \frac{(M(\infty) - \alpha)}{M(\infty)} \exp\left(-2k_+\left[\gamma(t - t_{maxP}) - \delta t_{maxP}(t - t_{maxP}) + \frac{1}{2}\delta(t^2 - t_{maxP}^2)\right]\right). \quad (52)$$

Interestingly, this form, including the $\sim t^2$ dependence, is similar to that found for infrangible systems described by Oosawa,[8,9,31] Eq. (24), but with an effective primary nucleation rate modified to account for the secondary nucleation process. Corrections to this form are given by forming a second iteration including $\mathcal{O}(k_n)$; the derivation of this is given in Appendix A and yields a highly accurate closed-form solution for the behaviour after the inflection point of $P(t)$. The second order result for $M(t)$, Eq. (A4), can be continued piecewise at t_{maxP} with the result for M_2^{series} from Eq. (43) to give a final result which is continuous by construction. The result is illustrated in Fig. 6 and written out fully up to third order terms in Appendix B, Eq. (B1).

Although these closed form solutions contain more terms than in the case where the secondary pathway is fragmentation, Eq. (20), it is interesting to note that the dependencies on the kinetic parameters are analogous. In particular, in the case of irreversible growth, $k_{off} = 0$, Eq. (A4) continued piecewise with Eq. (43) depends only upon the three kinetic parameters: κ, λ, and k_+. Additionally, in the absence of seed material, $M(0) = P(0) = 0$, the closed-form result depends only upon the two combinations of kinetic parameters: κ and λ.

C. Construction of a solution unifying both exponential and Oosawa type growth

The piecewise second-order solution discussed above and illustrated in Fig. 6 accounts explicitly for the change in behaviour at the inflection point in $P(t)$ and is highly accurate for all parameter values over the entire time course. In this section, we exploit our understanding of the two types of behaviour present in the system to construct a unified solution, resulting in a simplified closed-form solution in comparison to that given by Eq. (B1). In order to account for the change from exponential (Sec. V A) to Oosawa (Sec. V B) type behaviour in the polymer number concentration, $P(t)$, we construct an initial expression for the fixed point scheme with a form, $P_s(t)$, that is exact in both known limits of the polymer number concentration: $P_s(t) \xrightarrow{t \to 0} P_0(t)$ and $P_s(t) \xrightarrow{t \to \infty} P(\infty)$, where $P_0(t)$ is the early time linearized solution,[16,31] $P_0(t) = C_+ \kappa e^{\kappa t}/(2k_+) + C_- \kappa e^{-\kappa t}/(2k_+)$, and the long-time limit value of the polymer number, $P(\infty)$, is derived in Appendix C, Eq. (C6). These considerations yield

$$P_s(t) = \frac{P_0(t)}{1 + \frac{P_0(t)}{P(\infty)}}. \quad (53)$$

Performing a single fixed-point iteration by inserting Eq. (53) into Eq. (38) yields the first order self-consistent result for $M(t)$

$$\frac{M_s(t)}{M(\infty)} = 1 - \left(1 - \frac{M(0)}{M(\infty)}\right) \times \left(\frac{B_+ + C_+}{B_+ + C_+ e^{\kappa t}} \frac{B_- + C_+ e^{\kappa t}}{B_- + C_+}\right)^{\frac{k_\infty^2}{\kappa k_\infty}} e^{-k_\infty t}, \quad (54)$$

where the constants are given as

$$k_\infty = 2k_+ P(\infty) = \kappa \sqrt{\frac{2}{n_2(n_2+1)} + \frac{2}{n_c}\frac{\lambda^2}{\kappa^2} + \frac{2}{n_2}\frac{M(0)}{m(0)} + \left(\frac{2k_+ P(0)}{\kappa}\right)^2}, \quad (55)$$

$$\tilde{k}_\infty = \sqrt{k_\infty^2 - 4C_+ C_- \kappa^2}, \quad (56)$$

$$B_\pm = \frac{k_\infty \pm \tilde{k}_\infty}{2\kappa}. \quad (57)$$

This closed form result, which also applies for a system of fragmenting filaments as $n_2 \to 0$, has intermediate accuracy between the first-order solutions, Eqs. (3) and (37), and the highly accurate second order iterations, Eqs. (20) and (B1). The improvement in accuracy in comparison to the first order solution generally increases with n_2 as the inflection point in $P(t)$ moves to earlier times. Equation (54) has an accuracy with respect to the numerical solution of Eqs. (35) and (36) that is less in many cases than the experimental error of measurements of protein aggregation acquired using fluorometric or other optical methods commonly in use in biochemistry. The results, Eqs. (53) and (54), are illustrated in Fig. 7.

In the special case corresponding to frangible filaments, Eq. (53) reduces to the early time linearised solution $P_0(t)$;[31]

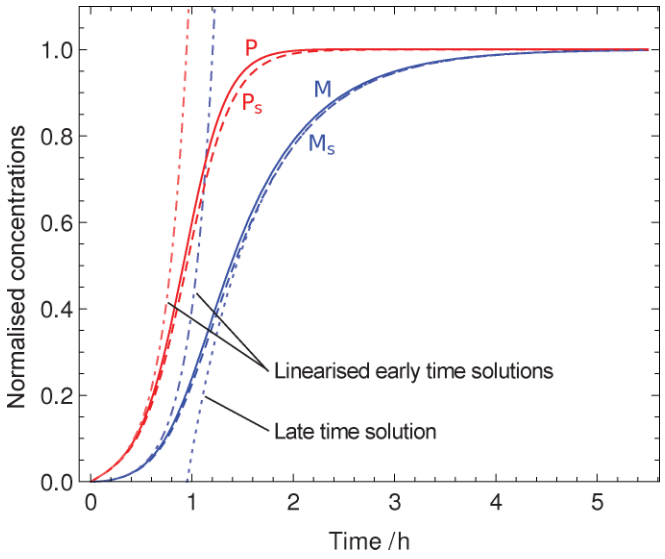

FIG. 7. The solutions for $P(t)$ and $M(t)$, Eqs. (53) and (54), constructed to include both exponential- and Oosawa-type behaviour. The results are plotted as $P(t)/P(\infty)$ and $M(t)/M(\infty)$, respectively. The solid lines show the exact numerical solution calculated from Eqs. (35) and (36), the dashed lines show Eqs. (53) and (54), and the dotted-dotted lines show the previously known linearized early time solutions (see Refs. 14–16, and 32). The blue dotted line shows the late time solution, Eq. (67). The parameters are $M(0) = P(0) = 0$, $k_+ = 5 \times 10^4$ M^{-1} s^{-1}, $k_{\rm off} = k_+ m_{\rm tot}/1000$, $k_2 m_{\rm tot}^{n_2} = 3 \times 10^{-7}$s^{-1}, $k_n m_{\rm tot}^{n_c - 1} = 3 \times 10^{-9}$ s^{-1}, $m_{\rm tot} = 5 \times 10^{-5}$ M, $n_c = 4$, $n_2 = 4$.

in this special case, therefore, the result $M_s(t)$ recovers exactly the first-order self-consistent solution for fragmenting filaments,[30,31] $M_1(t)$ Eq. (3). This limiting behaviour emerges since Eqs. (35) and (36) with $n_2 \to 0$ reproduce correctly the time evolution of the polymer mass concentration of fragmenting filaments, given from Eqs. (1) and (2), despite the fact that they fail to account exactly for the long-time limiting behaviour of the polymer number concentration.[31,35]

As a consistency check we verify that the early time limit of Eq. (54) reduces to the well-known linearised solution.[16,31] When the system is driven by secondary nucleation, the conditions $|B_+| \gg C_+$, $|B_-| \ll C_+$ with $\tilde{k}_\infty = k_\infty - 2C_+C_-\kappa^2/k_\infty + \mathcal{O}((C_+C_-\kappa^2)^2/k_\infty^2)$ yield the expansion for early times

$$\begin{aligned}
\frac{M_s(t)}{M(\infty)} &\approx 1 - \left(1 - \frac{M(0)}{M(\infty)}\right)\left[\left(1 + \frac{k_\infty^2}{\kappa\tilde{k}_\infty}\frac{C_+}{B_+}\right)\right. \\
&\quad \times \left(1 - \frac{k_\infty^2}{\kappa\tilde{k}_\infty}\frac{C_+}{B_+}e^{\kappa t}\right) e^{\frac{k_\infty^2}{\kappa\tilde{k}_\infty}\kappa t}\left(1 + \frac{k_\infty^2}{\kappa\tilde{k}_\infty}\frac{B_-}{C_+e^{\kappa t}}\right) \\
&\quad \left. \times \left(1 - \frac{k_\infty^2}{\kappa\tilde{k}_\infty}\frac{B_-}{C_+}\right)\right] e^{-k_\infty t} \\
&\approx 1 - \left(1 - \frac{M(0)}{M(\infty)}\right)\left[(1 + C_+)(1 - C_+e^{\kappa t})\right. \\
&\quad \left. \times (1 + C_-e^{-\kappa t})(1 - C_-)\right] \\
&= C_+(e^{\kappa t} - 1) - C_-(e^{-\kappa t} - 1) - \frac{M(0)}{M(\infty)} + \mathcal{O}(C_\pm^2) \\
&\quad + \mathcal{O}(C_\pm M(0)M(\infty)^{-1}). \qquad (58)
\end{aligned}$$

an expression that recovers exactly the early time linearized solution.[31]

The scaling behaviour of the lag-time may be found from Eq. (54). For a system dominated by secondary nucleation, beyond early times Eq. (54) becomes

$$\frac{M_s(t)}{M(\infty)} = 1 - \left(\frac{B_+ + C_+}{B_+ + C_+e^{\kappa t}}\right)^{\frac{k_\infty^2}{\kappa\tilde{k}_\infty}}, \qquad (59)$$

from which the time at the point of inflection in $M(t)$ is found to occur at

$$t_{\rm max} = \left[\log\left(\frac{1}{C_+}\right) - \log\left(\frac{k_\infty^2}{\kappa\tilde{k}_\infty B_+}\right)\right]\kappa^{-1} \approx \log\left(\frac{1}{C_+}\right)\kappa^{-1}, \qquad (60)$$

since the condition $n_c\kappa^2 \gg n_2(n_2+1)\lambda^2$ yields $B_+ \approx k_\infty/\kappa$ and $k_\infty \approx \tilde{k}_\infty$ for systems that are not heavily seeded. The maximal growth rate is then given as

$$\begin{aligned}
r_{\rm max} &= \frac{\frac{k_\infty^2}{\kappa\tilde{k}_\infty}}{1 + \frac{k_\infty^2}{\kappa\tilde{k}_\infty}}\left(\frac{(B_+ + C_+)\frac{k_\infty^2}{\kappa\tilde{k}_\infty}}{B_+\left(1 + \frac{k_\infty^2}{\kappa\tilde{k}_\infty}\right)}\right)^{\frac{k_\infty^2}{\kappa\tilde{k}_\infty}} M(\infty)\kappa, \qquad (61) \\
&\approx \frac{\theta}{1+\theta}\left(\frac{\theta}{1+\theta}\right)^{\theta} M(\infty)\kappa. \qquad (62)
\end{aligned}$$

The lag-time, defined in Eq. (25), may then be found as

$$\begin{aligned}
\tau_{\rm lag} &= \left(\log\left(\frac{1}{C_+}\right) - \log\left(\frac{k_\infty^2}{\kappa\tilde{k}_\infty B_+}\right)\right. \\
&\quad \left. - \frac{1 + \frac{k_\infty^2}{\kappa\tilde{k}_\infty}}{\frac{k_\infty^2}{\kappa\tilde{k}_\infty}}\left(\frac{B_+\left(1 + \frac{k_\infty^2}{\kappa\tilde{k}_\infty}\right)}{(B_+ + C_+)\frac{k_\infty^2}{\kappa\tilde{k}_\infty}}\right)^{\frac{k_\infty^2}{\kappa\tilde{k}_\infty}}\right)\kappa^{-1}, \qquad (63) \\
&\approx \left[\log\left(\frac{1}{C_+}\right) - \frac{1+\theta}{\theta}\left(\left(\frac{1+\theta}{\theta}\right)^{\theta} - 1\right)\right]\kappa^{-1}, \qquad (64)
\end{aligned}$$

where $k_\infty/\kappa \approx \theta = \sqrt{2/[n_2(n_2+1)]}$. These results Eqs. (62) and (64) recover the form of scaling laws previously identified in Eqs. (31), (34), and (44) and provide, in a simple closed form, expressions for the constant terms in the scaling laws valid for any $n_2 \geq 0$. In particular, the constant terms generated by Eq. (64) reproduce the constants found in Eq. (44) to within better than 10%. Moreover, for higher n_2, Eq. (64) offers an improvement over Eq. (44) in the accuracy

of this constant relative to the numerical solution. Remarkably, in the limit $n_2 \to 0$, the identity $e = \lim_{n\to\infty}(1+1/n)^n$ results in Eqs. (62) and (64) recovering exactly the scaling results from the first-order iteration.[30,31]

VI. TIME TO COMPLETION

The polymerization reaction comes to completion when the free monomer has been predominantly depleted, and an equilibrium is established between the aggregated and soluble phases. The time at which this equilibrium is reached depends on the initial concentration of monomer at the beginning of the reaction. We show here that this dependence is essentially a power-law of a form analogous to that governing the lag-time but with a different proportionality constant. We consider here the case where the overall reaction is driven by secondary nucleation processes, and the primary nucleation terms described by λ can be neglected in front of terms in κ.

For times $t \gg \kappa^{-1}$, Eqs. (20), (43), and (54) each show that (for any given n_2) the fractional polymer mass concentration is approximately a function only of the combination $C_+e^{\kappa t}$. As such, the time needed to reach each given fractional polymer mass concentration in this time limit must correspond to a constant value of $C_+e^{\kappa t}$. In particular, if the end point of the reaction is defined as τ_{end} such that $M(\tau_{\text{end}})/M(\infty) = s$, for some constant $s \to 1$, then it must be the case that $C_+e^{\kappa \tau_{end}}$ is constant. Explicitly, for any given n_2 there is a constant c such that $C_+e^{\kappa\tau_{\text{end}}} = c$, which yields the expression

$$\tau_{\text{end}} = \left[\log(1/C_+) + \log(c)\right]\kappa^{-1}. \tag{65}$$

Interestingly, since $C_+e^{\kappa\tau_{\text{end}}}$ is approximately a constant that is independent of the kinetic parameters, the number of terms required in the summations in Eqs. (20) and (43), for convergence up to an appropriate s, must also be independent of the parameters.

A closed form expression for $\log(c)$ may be derived from Eq. (54). For a secondary nucleation dominated system beyond early times, Eq. (59) can be inverted to yield the time for the reaction end-point as

$$\tau_{\text{end}} = \left[\log(1/C_+) + \log(\theta[(1-s)^{-\frac{1}{\theta}} - 1])\right]\kappa^{-1}, \tag{66}$$

where $k_\infty/\kappa \approx \theta = \sqrt{2/[n_2(n_2+1)]}$ for a system dominated by secondary nucleation, $n_c\kappa^2 \gg n_2(n_2+1)\lambda^2$, and for small levels of initial seeding. Equation (66) has the expected form from Eq. (65) and identifies the constant term c as a function of the secondary nucleation exponent n_2. This scaling result is valid for all $n_2 \geq 0$, with $n_2 = 0$ recovering the end-point scaling predicted by the first-order result for the case of fragmenting filaments.[30,31] The result in the case of fragmenting filaments may, in particular, be improved by inverting the result of the second-order iteration Eq. (26) and solving the resulting polynomial equation for c.

It is interesting to note from Eq. (59) that as the exponential term becomes large at later times, $C_+e^{\kappa t} \gg B_+$, the polymer mass concentration evolves as

$$\frac{M_s(t)}{M(\infty)} \approx 1 - \frac{B_+}{C_+}e^{-k_\infty t}. \tag{67}$$

The fractional polymer mass concentration at which this occurs depends on n_2 (since $B_+ \approx \theta$), with the condition $C_+e^{\kappa t} \gg B_+$ being equivalent to $M(t)/M(\infty) \gg 1 - 2^{-\theta}$. This result shows that the transition to this long-time behaviour, Eq. (67), occurs at lower polymer mass concentrations for higher exponents n_2. Qualitatively, this behaviour is expected since, for $n_2 > 1$, the elongation rate has the weakest monomer dependency in the system. For $n_2 = 0$, this regime is not reached, with the condition reading $M(t)/M(\infty) \gg 1$, since the secondary pathway in the case of fragmenting filaments has a weaker monomer dependency than the elongation rate.

As an illustrative example, we provide explicitly the scaling laws for the time to 99.9% completion for various values of n_2

$$\tau_{\text{end}} = \begin{cases} \left[\log(1/C_+) + 3.0\right]\kappa^{-1} & \text{fragmentation} \\ \left[\log(1/C_+) + 6.9\right]\kappa^{-1} & n_2 = 1 \\ \left[\log(1/C_+) + 11\right]\kappa^{-1} & n_2 = 2 \\ \left[\log(1/C_+) + 25\right]\kappa^{-1} & n_2 = 5 \\ \left[\log(1/C_+) + 49\right]\kappa^{-1} & n_2 = 10 \end{cases}, \tag{68}$$

which are similar in form to the lag time scaling Eq. (44). This scaling is also of practical interest as it allows the prediction of the relevant timescale of a reaction at the design stage of experiments. In particular, the scaling law reveals approximately $\tau_{\text{end}} \sim m(0)^{-\frac{n_2+1}{2}}$, which is useful in predicting the relevant timescales of reactions at different total monomer concentrations.

VII. SELF-CONSISTENT SOLUTION FOR THE LENGTH DISTRIBUTION

We have derived earlier[31] the time evolution of the mean and standard deviation of the length distribution of fragmenting filaments in the case of a constant monomer concentration.[31] In the case of the standard deviation, these results were obtained for a system where all of the material was initially soluble under the assumption that the distribution is not heavily skewed. The availability of expressions for both the mean and the standard deviation makes it possible to evaluate the time evolution of the full filament length distribution within a self-consistent framework and determine the skewness and higher central moments of the length distribution. To this effect, we demonstrate the wider applicability and power of our self-consistent approach by finding the first correction to the symmetric Gaussian approximation to the length distribution using a self-consistent scheme. We use this result to determine the correction, relative to the mean, to the time evolution of the mode of the distribution, which is not available simply through knowledge of the first three moments of the distribution.

Formally integrating the master equation[31] for the irreversible growth of fragmenting filaments, the solution for the

full length distribution can be written as

$$f(t,j) = 2m_{\text{tot}}k_+ e^{-2m_{\text{tot}}k_+ t}\int_0^t e^{2m_{\text{tot}}k_+\tau} f(\tau, j-1)d\tau - k_- e^{-2m_{\text{tot}}k_+ t}\int_0^t e^{2m_{\text{tot}}k_+\tau}\left[(j-1)f(t,j) - 2\sum_{i=j+1}^{\infty} f(t,i)\right]d\tau + k_n m_{\text{tot}}^{n_c}\delta_{j,n_c}e^{-2m_{\text{tot}}k_+ t} \times \int_0^t e^{2m_{\text{tot}}k_+\tau}d\tau. \quad (69)$$

We note that it is possible to solve this equation exactly for any $f(j,t)$ recursively beginning with $f(t,n_c)$ and integrating $j-n_c$ times. However, given the considerable coupling of equations in this system through the summation term relating to filament breakage, this approach becomes impractical beyond small j. Instead, it is possible to remove the coupling originating in the fragmentation related terms using a self-consistent approach.

Consider initially the master equation without filament fragmentation, $k_- = 0$. In this case each equation is only coupled to its nearest neighbours and the solution $f_{k_-=0}(j,t)$, found by repeated integration, is given as

$$\frac{f_{k_-=0}(j,t)}{P(t)} = \frac{k_n m_{\text{tot}}^{n_c-1}}{2k_+}(1-e^{-2m_{\text{tot}}k_+ t}) - \frac{k_n m_{\text{tot}}^{n_c-1}}{2k_+}e^{-2m_{\text{tot}}k_+ t}\sum_{i=1}^{j-n}\frac{(2m_{\text{tot}}k_+ t)^i}{i!}. \quad (70)$$

In this case the master equation is a discretization of an advection equation and so the solution describes a travelling wave in j moving to encompass larger filament sizes at velocity $2k_+m_{\text{tot}}$.

We now account in a self-consistent manner for the terms in the master equation describing fragmentation by introducing for the filament length distribution in these terms the Gaussian approximation with mean[31] $\mu(t)$ and standard deviation[31] $\mu(t)/\sqrt{3}$

$$f_0(j,t) = \sqrt{\frac{3}{2\pi}}\frac{e^{-\frac{3(j-\mu(t))^2}{2\mu(t)^2}}}{\mu(t)}\frac{P(t)}{E_\infty}, \quad (71)$$

where E_∞ is a normalization constant for the distribution between $j=n_c$ and $j=\infty$, $E_\infty \approx 1/2(1+\text{erf}(\sqrt{3/2})) \approx 0.96$, where the approximation is valid since $\mu(t) \gg n_c$. Note that the distribution $f_0(j,t)$, due to the cut-off at n_c, has a mean length, $\mu_0(t)$, different to the exact value, $\mu(t)$

$$\mu_0(t) = \int_{n_c}^{\infty} s\frac{f_0(s,t)}{P(t)}ds = \mu(t) + \frac{1}{3}\mu(t)^2\frac{f_0(n_c,t)}{P(t)}. \quad (72)$$

We now consider the breakage related terms in Eq. (69). Introducing the initial Gaussian approximation and replacing the summation term in Eq. (69) with a continuum approximation leaves

$$-k_- e^{-2m_{\text{tot}}k_+ t}\int_0^t e^{2m_{\text{tot}}k_+\tau}\left[(j-1)f_0(t,j) - 2P(t) + 2\times\int_{n_c}^{j} f_0(t,i)di\right]d\tau. \quad (73)$$

In addition, we must account for the coupling of these breakage related terms to nearest neighbours through the first term in Eq. (69), which introduces a summation over j. This allows us to write within this self-consistent framework the full length distribution as a function of time

$$f_1(j,t) = f_{k_-=0} - k_- e^{-2m_{\text{tot}}k_+ t}\int_{n_c}^{j}\int_0^t e^{2m_{\text{tot}}k_+\tau} \times\left[(s-1)f_0(t,j) - 2P(t) + 2\int_{n_c}^{s} f_0(t,i)di\right]d\tau ds. \quad (74)$$

Performing the integration with respect to time using the general expansion for large α, $e^{-\alpha t}\int_0^t e^{\alpha x}y(x)dx = y(t)/\alpha + \mathcal{O}(y'(t)/\alpha^2)$, allows us to evaluate these integrals to first-order approximation to give a new expression for the filament length distribution

$$f_1(j,t) = f_{k_-=0} + \frac{k_-}{2m_{\text{tot}}k_+}(2P(t)(j-n_c) - 2F_1(j,t) - F_2(j,t)), \quad (75)$$

where the functions $E(j,t)$, $F_1(j,t)$, and $F_2(j,t)$ are given in terms of error functions

$$E(j,t) = \int_{n_c}^{j} f_0(s,t)ds = \frac{P(t)}{2E_\infty}\left[-\text{erf}\left(\frac{\sqrt{\frac{3}{2}}(\mu(t)-j)}{\mu(t)}\right) + \text{erf}\left(\sqrt{\frac{3}{2}}\right)\right], \quad (76)$$

$$F_1(j,t) = \int_{n_c}^{j} E(s,t)ds = \int_{n_c}^{j}\int_{n_c}^{s} f_0(r,t)drds = [j-\mu(t)]E(j,t) + \frac{1}{3}\mu(t)^2[f_0(j,t) - f_0(n_c,t)], \quad (77)$$

$$F_2(j,t) = \int_{n_c}^{j}(s-1)f_0(s,t)ds = [\mu(t)-1]E(j,t) - \frac{1}{3}\mu(t)^2[f_0(j,t) - f_0(n_c,t)]. \quad (78)$$

For large j, the errors $\mathcal{O}(\alpha^{-2})$ accumulate due to the integral over j in Eq. (74), resulting in excellent accuracy for small and intermediate j but an incorrect limit for $j \to \infty$. This limit, however, can be evaluated exactly, yielding $P(t)[\mu_0(t) - 2n_c + 1]$. Removing the associated terms in

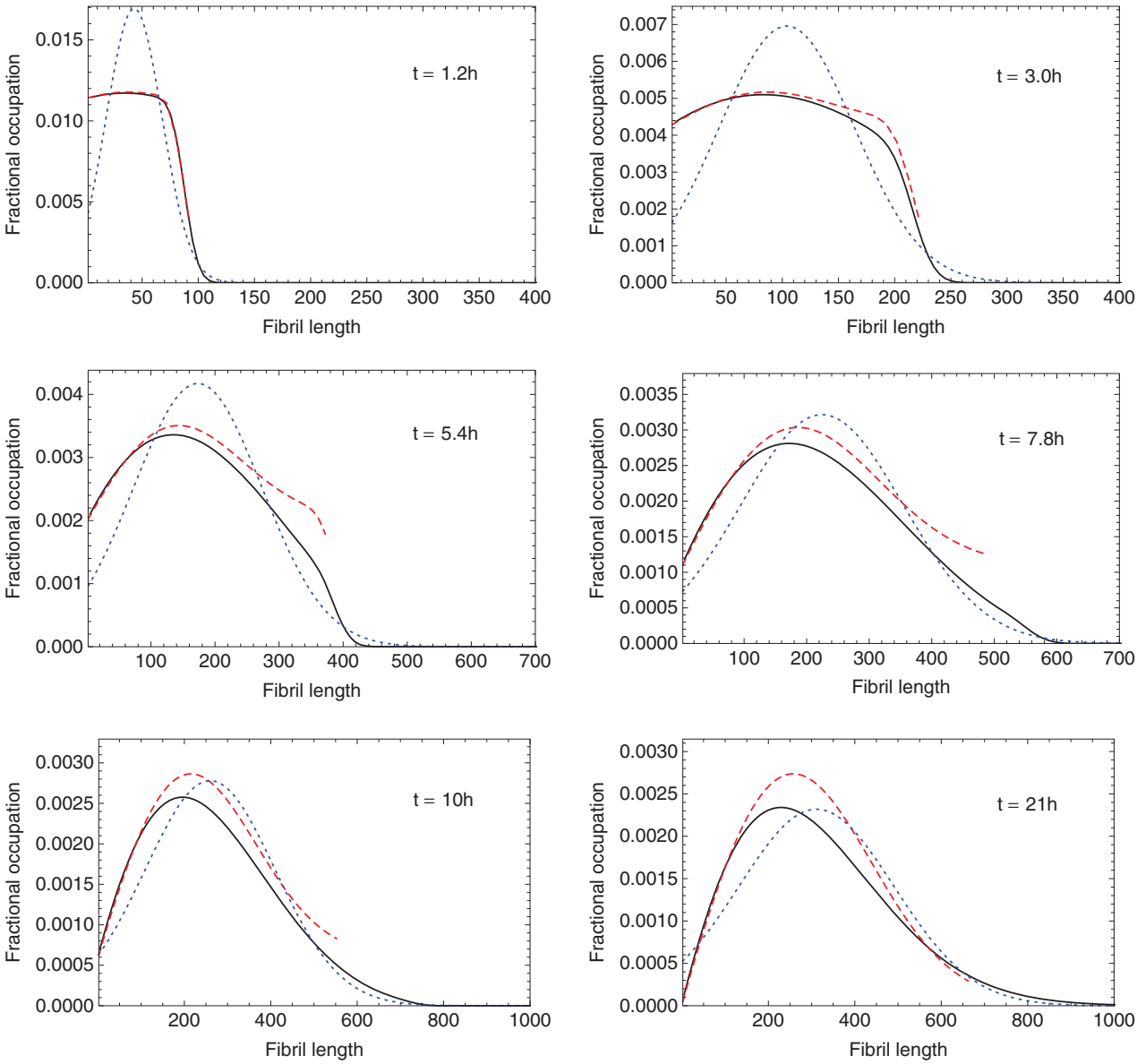

FIG. 8. The solution derived for the time evolution of the full filament length distribution in our self-consistent scheme, Eq. (79), is shown in red (dashed). The numerical result is shown in black, and the initial Gaussian approximation, Eq. (71), is shown in blue (dotted). The parameters are $M(0) = P(0) = 0$, $k_+ = 1 \times 10^4\ \mathrm{M}^{-1}\ \mathrm{s}^{-1}$, $k_{\mathrm{off}} = 0$, $k_- = 2 \times 10^{-7}\mathrm{s}^{-1}$, $k_n = 1 \times 10^{-5}\ \mathrm{M}^{-1}\ \mathrm{s}^{-1}$, $m_{\mathrm{tot}} = 1 \times 10^{-6}\ \mathrm{M}$, $n_c = 2$.

Eq. (75) yields

$$f_1(j,t) = f_{k_-=0} + \frac{k_-}{2m_{\mathrm{tot}}k_+}\left[2[P(t) - E(j,t)][j - n_c] - \frac{1}{3}\mu(t)^2\left[f_0(j,t) - \left[1 - \frac{E(j,t)}{P(t)}\right]f_0(n_c,t)\right]\right], \tag{79}$$

where $f_{k_-=0}$ is given in Eq. (70). The result $f_1(j,t)$, Eq. (79), is expected to be highly accurate for small filament sizes, since the coupled integration over j is most accurate in this regime. Due to the contribution from the solution of the advection equation, Eq. (70), we would expect the result to be accurate up to lengths $2\mu(t)$, or equivalently $\sqrt{3} \approx 1.7$ standard deviations above the mean, thus being accurate for all but the tail of the distribution. The improvement over the initial Gaussian solution obtained using the information from the first three principal moments is shown in Fig. 8.

The mode of the distribution can be obtained from the condition $\partial f/\partial j|_{j=j_{\mathrm{mode}}} = 0$, resulting in

$$0 = f_0(j_{\mathrm{mode}},t)(2n_c - \mu_0(t) - j) + 2P(t) - 2E(j_{\mathrm{mode}},t), \tag{80}$$

since $(\mu(t)^2/[3f_0(j,t)])\partial f_0/\partial j = \mu(t) - j$. Expanding the Gaussian $f_0(j,t)$ to lowest order about the mean results in

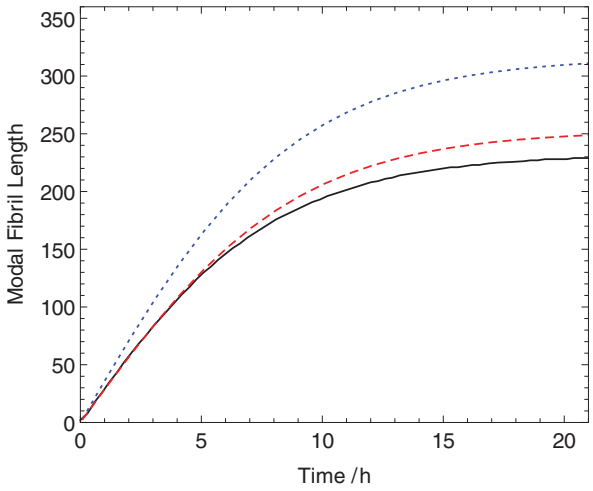

FIG. 9. The correction to the mode in relation to the mean, Eq. (82), exhibited by our solution to the full length distribution, Eq. (79), is shown in red (dashed). The numerical result is shown in black, and the result from the initial Gaussian approximation is shown in blue (dotted). The parameters are the same as in Fig. 8.

$$0 = \frac{\sqrt{\frac{3}{2\pi}}}{\mu(t)E_\infty}[2n_c - \mu_0(t) - j_{\text{mode}}] + 2 - 2\left(\frac{1}{2E_\infty}\text{erf}\left(\sqrt{\frac{3}{2}}\frac{\mu(t)-n_c}{\mu(t)}\right) + \frac{\sqrt{\frac{3}{2\pi}}}{\mu(t)E_\infty}[j_{\text{mode}} - \mu(t)]\right) + \mathcal{O}(j^2). \quad (81)$$

Using $\mu(t) \gg n_c$ and Eqs. (71) and (72) yields the simple result

$$j_{\text{mode}} = \frac{1}{3}\left(1 + \sqrt{\frac{2\pi}{3}} - \frac{1}{3}\sqrt{\frac{3}{2\pi}}\frac{e^{-\frac{3}{2}}}{E_\infty}\right)\mu(t) \approx 0.8\mu(t). \quad (82)$$

As expected, the mode of the distribution is below the mean, and we recover the interesting result that the ratio of the mode to the mean, and hence also to the standard deviation, is approximately a constant in time for this system; the mode evolves with the same functional form as the mean and standard deviation. The improvement in the value of the mode of the filament distribution in the distribution $f_1(j,t)$ compared with the original Gaussian $f_0(j,t)$ is shown in Fig. 9.

VIII. CONCLUSION

We have used the power of iterative fixed point schemes to provide self-consistent solutions to growth processes described by highly non-linear master equations. We have shown that corrections to the scaling behaviour emerging from first order results can be well captured by second order self-consistent solutions, which yield coefficients for the characteristic scaling laws which are very close to ones obtained from numerical evaluation. More generally, these results illustrate the value of fixed-point analysis strategies in order to provide self-consistent solutions to complex growth problems beyond perturbative treatments.

APPENDIX A: SECOND ORDER ITERATION POST-INFLECTION POINT

The first post-inflection point self-consistent solution for the moment $P(t)$ is found by inserting $M_1^{t_{\text{maxP}}}$ from Eq. (52) into Eq. (35); crucially, we include here exactly the term $\mathcal{O}(k_n)$. Together with the condition $P(t_{\text{maxP}}) = \gamma$ this yields

$$P_1^{t_{\text{maxP}}}(t) = \gamma + k_2 m_{\text{tot}} \text{h}(n_2, t) - k_2 \text{h}(n_2+1, t) + k_n \text{h}(n_c, t), \quad (A1)$$

where

$$\text{h}(x,t) = \frac{e^{\frac{\gamma}{\delta}k_+\gamma x}\sqrt{\pi}(\text{er}(x,t) - \text{er}(x, t_{\text{maxP}}))(m_{\text{tot}} - \alpha)^x}{2\sqrt{k_+\delta x}}, \quad (A2)$$

and

$$\text{er}(z,t) = \text{erf}\left(\frac{\gamma}{\delta}\sqrt{k_+\delta z} + (t - t_{\text{maxP}})\sqrt{k_+\delta z}\right), \quad (A3)$$

for the error function $\text{erf}(z) = 2/\sqrt{\pi}\int_0^z e^{-t^2}dt$. A further iteration can be performed from Eq. (36) by direct integration, yielding the final result for the post-inflection point solution $M_2^{t_{\text{maxP}}}$

$$\frac{M_2^{t_{\text{maxP}}}(t)}{M(\infty)} = 1 - \frac{(M(\infty) - \alpha)}{M(\infty)}\exp\Big[-2k_+\gamma(t - t_{\text{max}}) - \kappa_0^2 \text{v}(n_2, t)\frac{m_{\text{tot}}}{m(0)} + \kappa_0^2 \text{v}(n_2+1, t) - \lambda^2 \text{v}(n_c, t)\Big], \quad (A4)$$

where

$$\text{v}(x,t) = \left(\frac{\gamma}{\delta} + (t - t_{\text{maxP}})\right)\frac{\text{h}(x,t)}{m(0)^x} + \frac{e^{-k_+\delta x(t-t_{\text{maxP}})^2 - 2k_+\gamma x(t-t_{\text{maxP}})} - 1}{2k_+\delta x}\frac{(m_{\text{tot}} - \alpha)^x}{m(0)^x}, \quad (A5)$$

for $\kappa_0 = \kappa|_{k_{\text{off}}=0} = \sqrt{2m(0)^{n_2+1}k_+k_2}$. Apart from the influence of the boundary conditions defined by α and β, these results for M, Eqs. (52) and (A4), depend on the rate constants only through the combinations $k_+\gamma$, $k_+\delta$ and their ratio γ/δ. These combinations are given approximately as

$$k_+\gamma \approx \frac{k_+\dot{M}_2(t_{\text{maxP}})}{2(k_+m_2(t_{\text{maxP}}) - k_{\text{off}})}, \quad (A6)$$

$$k_+\delta = \frac{M_2(t_{\text{maxP}})m_2(t_{\text{maxP}})^{n_2}}{2m(0)^{n_2+1}}\kappa_0^2 + \frac{m_2(t_{\text{maxP}})^{n_c}}{2m(0)^{n_c}}\lambda^2. \quad (A7)$$

We note that due to the explicit inclusion of primary nucleation terms, we recover the combination λ which is the single parameter that defines growth of filaments in the absence of secondary nucleation.[9,31] These terms governed by λ in Eq. (A4) become important for kinetic parameters that result in primary nucleation being more significant than secondary nucleation for creating seeds for times after t_{maxP}. In many cases, particularly for $n_c > n_2$, these terms are not significant.

APPENDIX B: FULL SECOND-ORDER SOLUTION FOR MONOMER-DEPENDENT SECONDARY NUCLEATION

The second-order self-consistent solution to Eqs. (35) and (36) for the polymer mass concentration of a system of filaments growing through primary nucleation, monomer addition, monomer dissociation, and secondary nucleation derived in this paper can be written out in full as

$$\frac{M(t)}{M(\infty)} = \begin{cases} 1 - \exp\Big\{ -(e^{\kappa t}-1)C_+ + (e^{-\kappa t}-1)C_- \\ \quad + \dfrac{\left((1+n_2)^2 - n_2^2\right)}{8}[(e^{2t\kappa} - 1 - \pi_+^{(2)}(t))C_+^2 + (e^{-2t\kappa} - 1 - \pi_-^{(2)}(t))C_-^2] & t \le t_{\mathrm{maxP}} \\ \quad + \dfrac{\left((1+n_2)^3 - n_2^3\right)}{54}[-(e^{3t\kappa} - 1 - \pi_+^{(3)}(t))C_+^3 + (e^{-3t\kappa} - 1 - \pi_-^{(3)}(t))C_-^3] - \dfrac{M(0)}{M(\infty)} \Big\} \\ 1 - \dfrac{(M(\infty) - M(t_{\mathrm{maxP}}))}{M(\infty)} \exp\Big[-2k_+\gamma(t - t_{\max}) - \kappa_0^2 \mathrm{v}(n_2,t)\dfrac{m_{\mathrm{tot}}}{m(0)} + \kappa_0^2 \mathrm{v}(n_2+1,t) - \lambda^2 \mathrm{v}(n_c,t) \Big] & t > t_{\mathrm{maxP}}, \end{cases} \tag{B1}$$

where the dependencies on the rate constants and initial conditions are defined through

$$\pi_\pm^{(2)}(t) = \pm 2\kappa t + 2\kappa^2 t^2 + (\pm 4\kappa^3 t^3/3 + 2\kappa^4 t^4/3)\left\{1 - 1/\left[(1+n_2)^2 - n_2^2\right]\right\}, \tag{B2}$$

$$\pi_\pm^{(3)}(t) = \pm 3\kappa t + 9\kappa^2 t^2/2 \pm 9\kappa^3 t^3/2 + 27\kappa^4 t^4/8 + (\pm 81\kappa^5 t^5/40 + 81\kappa^6 t^6/80)\left\{1 - 1/\left[(1+n_2)^3 - n_2^3\right]\right\}, \tag{B3}$$

$$\kappa = \sqrt{2(k_+ m(0) - k_{\mathrm{off}})m(0)^{n_2} k_2} \quad \kappa_0 = \sqrt{2m(0)^{n_2+1} k_+ k_2} \quad \lambda = \sqrt{2m(0)^{n_c} k_+ k_n}, \tag{B4}$$

$$C_\pm = \frac{k_+ P(0)}{\kappa} \pm \frac{k_+ M(0)}{2[m(0)k_+ - k_{\mathrm{off}}]} \pm \frac{\lambda^2}{2\kappa^2} \qquad b = \log\left(\frac{m_*}{m(0)}\right) - \frac{\lambda^2}{\kappa^2} + \frac{M(0)}{M(\infty)} - \frac{k_+ M(0)}{k_+ m(0) - k_{\mathrm{off}}}, \tag{B5}$$

$$M(\infty) = m_{\mathrm{tot}} - k_{\mathrm{off}}/k_+ \qquad m_* = \eta - \frac{\lambda^2 \eta^{n_c-1} n_c}{\lambda^2 n_c (n_c - 1)\eta^{n_c-2} - \kappa_0^2 n_2 \eta^{n_2-2} m_{\mathrm{tot}} m(0)^{n_c-n_2-1}} \qquad \eta = m_{\mathrm{tot}} n_2/(1+n_2), \tag{B6}$$

$$t_{\mathrm{maxP}} = \begin{cases} 0 & m_* > m(0) \text{ or } (1+n_2)\kappa_0^2[m(0) - \eta] < n_c m(0)\lambda^2, \\ \kappa^{-1} \log\left(\frac{-b + \sqrt{b^2 + 4C_+C_-}}{2C_+}\right) & \text{otherwise} \end{cases} \tag{B7}$$

$$\mathrm{h}(x,t) = \frac{e^{\frac{\gamma}{\delta}k_+\gamma x}\sqrt{\pi}(\mathrm{er}(x,t) - \mathrm{er}(x,t_{\mathrm{maxP}}))\,(m_{\mathrm{tot}} - M(t_{\mathrm{maxP}}))^x}{2\sqrt{k_+\delta x}} \qquad \mathrm{er}(z,t) = \mathrm{erf}\left(\frac{\gamma}{\delta}\sqrt{k_+\delta z} + (t - t_{\mathrm{maxP}})\sqrt{k_+\delta z}\right), \tag{B8}$$

$$\mathrm{v}(x,t) = \left(\frac{\gamma}{\delta} + (t - t_{\mathrm{maxP}})\right)\frac{\mathrm{h}(x,t)}{m(0)^x} + \frac{e^{-k_+\delta x(t - t_{\mathrm{maxP}})^2 - 2k_+\gamma x(t - t_{\mathrm{maxP}})} - 1}{2k_+\delta x}\frac{(m_{\mathrm{tot}} - M(t_{\mathrm{maxP}}))^x}{m(0)^x}, \tag{B9}$$

$$k_+\gamma \approx \frac{k_+\dot{M}_2(t_{\mathrm{maxP}})}{2(k_+m_2(t_{\mathrm{maxP}})-k_{\mathrm{off}})} \quad k_+\delta = \frac{M_2(t_{\mathrm{maxP}})m_2(t_{\mathrm{maxP}})^{n_2}}{2m(0)^{n_2+1}}\kappa_0^2 + \frac{m_2(t_{\mathrm{maxP}})^{n_c}}{2m(0)^{n_c}}\lambda^2. \tag{B10}$$

The accuracy of this solution even for high exponents n_2 and n_c is demonstrated in Fig. 2.

APPENDIX C: POLYMER NUMBER CONCENTRATION IN THE LONG-TIME LIMIT

For the case of fragmenting filaments, the long-time polymer number concentration is given approximately from the differential equation system Eqs. (1) and (2) as[35]

$$P(\infty) = \frac{M(\infty)}{2n_c - 1} \qquad \text{fragmentation.} \tag{C1}$$

For the case of monomer-dependent secondary nucleation, consider Eqs. (35) and (36) in the limit of no depolymerisation rate $k_{\mathrm{off}} = 0$. Obtaining dm/dt from Eq. (36) via conservation of mass and then dividing through by $m(t)$, differentiating, and substituting from Eq. (35) leaves an equation in terms of $m(t)$ only

$$\frac{d^2\log(m(t))}{dt^2} = -2k_+k_nm(t)^{n_c} - 2k_+k_2m_{\mathrm{tot}}m(t)^{n_2} + 2k_+k_2m(t)^{n_2+1}. \tag{C2}$$

Multiplying both sides by $d\log(m(t))/dt = 1/m\ dm/dt$ and re-writing terms results in

$$\frac{1}{2}\frac{d}{dt}\left(\frac{d\log(m(t))}{dt}\right)^2 = \frac{d}{dt}\left(-\frac{2k_+k_nm(t)^{n_c}}{n_c} - \frac{2k_+k_2m_{\mathrm{tot}}m(t)^{n_2}}{n_2} + \frac{2k_+k_2m(t)^{n_2+1}}{n_2+1}\right). \tag{C3}$$

Integrating and rearranging results in the first-order differential equation for $m(t)$

$$\frac{1}{m}\frac{dm}{dt} = -\left[\tilde{\kappa}^2 - \frac{4k_+k_nm(t)^{n_c}}{n_c} - \frac{4k_+k_2m_{\mathrm{tot}}m(t)^{n_2}}{n_2} + \frac{4k_+k_2m(t)^{n_2+1}}{n_2+1}\right]^{1/2}, \tag{C4}$$

where the constant

$$\tilde{\kappa}^2 = (2k_+P(0))^2 + \frac{4k_+k_nm(0)^{n_c}}{n_c} + \frac{4k_+k_2m_{\mathrm{tot}}m(0)^{n_2}}{n_2} - \frac{4k_+k_2m(0)^{n_2+1}}{n_2+1}, \tag{C5}$$

is given from the initial conditions. Considering Eq. (C4) as $t \to \infty$, and using $1/m\,dm/dt = -2k_+P(t)$ and $m(\infty) = 0$, the long-time limit polymer number concentration, in the absence of a depolymerisation rate, is found in closed form as

$$P(\infty) = \frac{\tilde{\kappa}}{2k_+} \qquad n_2 > 0. \tag{C6}$$

This result is exact in the absence of depolymerisation and applies approximately over the timescale of the polymerisation kinetics $\sim\kappa^{-1}$ even in the presence of a small depolymerisation rate $k_{\mathrm{off}} \ll k_+m_{\mathrm{tot}}$. However, even small values of the depolymerisation rate lead, over a significantly longer timescale $t \gg \kappa^{-1}$, to a diffusive-like redistribution in the long-time limit length distribution of filaments. This results in Eq. (C6) describing the transient state at the end of the polymerisation reaction prior to this relaxation; this final redistribution is discussed in Ref. 35.

[1] S. R. Collins, A. Douglass, R. D. Vale, and J. S. Weissman, PLoS Biol. **2**, e321 (2004).
[2] W.-F. Xue, S. W. Homans, and S. E. Radford, Proc. Natl. Acad. Sci. U.S.A. **105**, 8926 (2008).
[3] T. P. J. Knowles, T. W. Oppenheim, A. K. Buell, D. Y. Chirgadze, and M. E. Welland, Nat. Nanotechnol. **5**, 204 (2010).
[4] A. M. Ruschak and A. D. Miranker, Proc. Natl. Acad. Sci. U.S.A. **104**, 12341 (2007).
[5] K. C. Kunes, D. L. Cox, and R. R. P. Singh, Phys. Rev. E **72**, 051915 (2005).
[6] E. T. Powers and D. L. Powers, Biophys. J. **94**, 379 (2008).
[7] A. M. Morris, M. A. Watzky, and R. G. Finke, Biochim. Biophys. Acta. **1794**, 375 (2009).
[8] F. Oosawa and M. Kasai, J. Mol. Biol. **4**, 10 (1962).
[9] F. Oosawa and S. Asakura, *Thermodynamics of the Polymerization of Protein* (Academic, New York, 1975).
[10] A. Wegner, J. Mol. Biol. **161**, 217 (1982).
[11] A. Wegner, Nature (London) **296**, 266 (1982).
[12] L. S. Tobacman and E. D. Korn, J. Biol. Chem. **258**, 3207 (1983).
[13] F. A. Ferrone, J. Hofrichter, and W. A. Eaton, J. Mol. Biol. **183**, 591 (1985).
[14] J. Hofrichter, P. D. Ross, and W. A. Eaton, Proc. Natl. Acad. Sci. U.S.A. **71**, 4864 (1974).
[15] F. A. Ferrone, J. Hofrichter, H. R. Sunshine, and W. A. Eaton, Biophys. J. **32**, 361 (1980).
[16] F. A. Ferrone, J. Hofrichter, and W. A. Eaton, J. Mol. Biol. **183**, 611 (1985).
[17] C. M. Dobson, Nature (London) **418**, 729 (2002).
[18] J. Hardy and D. J. Selkoe, Science **297**, 353 (2002).
[19] C. M. Dobson, Nature (London) **426**, 884 (2003).
[20] F. Chiti and C. M. Dobson, Annu. Rev. Biochem. **75**, 333 (2006).
[21] D. J. Selkoe, Nature (London) **426**, 900 (2003).
[22] W. Dauer and S. Przedborski, Neuron **39**, 889 (2003).
[23] S. B. Prusiner, Science **252**, 1515 (1991).
[24] A. Aguzzi and C. Haass, Science **302**, 814 (2003).
[25] M. Tanaka, S. R. Collins, B. H. Toyama, and J. S. Weissman, Nature (London) **442**, 585 (2006).
[26] D. Hall and H. Edskes, J. Mol. Biol. **336**, 775 (2004).
[27] W.-F. Xue, A. L. Hellewell, W. S. Gosal, S. W. Homans, E. W. Hewitt, and S. E. Radford, J. Biol. Chem. **284**, 34272 (2009).
[28] J. T. Jarrett and P. T. Lansbury, Cell **73**, 1055 (1993).

[29]M. A. Nowak, D. C. Krakauer, A. Klug, and R. M. May, Integr. Biol. **1**, 3 (1998).
[30]T. P. J. Knowles, C. A. Waudby, G. L. Devlin, S. I. A. Cohen, A. Aguzzi, M. Vendruscolo, E. M. Terentjev, M. E. Welland, and C. M. Dobson, Science **326**, 1533 (2009).
[31]S. I. A. Cohen, M. Vendruscolo, C. M. Dobson, E. M. Terentjev, and T. P. J. Knowles, J. Chem. Phys. **135**, 065105 (2011).
[32]F. Ferrone, Methods Enzymol. **309**, 256 (1999).
[33]J. Masel, V. A. Jansen, and M. A. Nowak, Biophys. Chem. **77**, 139 (1999).
[34]T. Poeschel, N. V. Brilliantov, and C. Froemmel, Biophys. J. **85**, 3460 (2003).
[35]S. I. A. Cohen, M. Vendruscolo, C. M. Dobson, and T. P. J. Knowles, J. Chem. Phys. **135**, 065107 (2011).
[36]M. F. Bishop and F. A. Ferrone, Biophys. J. **46**, 631 (1984).
[37]B. D. Ganapol, e-print arXiv: 1006.3022 (2010).